
UNLEASH THE POWER OF ELLIPSIS: ACCURACY-ENHANCED SPARSE VECTOR TECHNIQUE WITH EXPONENTIAL NOISE

A PREPRINT

Yuhan Liu
Renmin University of China
liuyh2019@ruc.edu.cn

Sheng Wang
Alibaba Group
sh.wang@alibaba-inc.com

Yixuan Liu
Remin University of China
liuyixuan@ruc.edu.com

Feifei Li
Alibaba Group
lifeifei@alibaba-inc.com

Hong Chen
Renmin university of China
chong@ruc.edu.cn

July 30, 2024

ABSTRACT

The Sparse Vector Technique (SVT) is one of the most fundamental tools in differential privacy (DP). It works as a backbone for adaptive data analysis by answering a sequence of queries on a given dataset, and gleaming useful information in a privacy-preserving manner. Unlike the typical private query releases that directly publicize the noisy query results, SVT is less informative—it keeps the noisy query results to itself and only reveals a binary bit for each query, indicating whether the query result surpasses a predefined threshold. To provide a rigorous DP guarantee for SVT, prior works in the literature adopt a *conservative* privacy analysis by assuming the direct disclosure of noisy query results as in typical private query releases. This approach, however, hinders SVT from achieving higher query accuracy due to an overestimation of the privacy risks, which further leads to an excessive noise injection using the Laplacian or Gaussian noise for perturbation. Motivated by this, we provide a new privacy analysis for SVT by considering its less informative nature. Our analysis results not only broaden the range of applicable noise types for perturbation in SVT, but also identify the exponential noise as optimal among all evaluated noises (which, however, is usually deemed non-applicable in prior works). The main challenge in applying exponential noise to SVT is mitigating the sub-optimal performance due to the bias introduced by noise distributions. To address this, we develop a utility-oriented optimal threshold correction method and an appending strategy, which enhances the performance of SVT by increasing the precision and recall, respectively. The effectiveness of our proposed methods is substantiated both theoretically and empirically, demonstrating significant improvements up to 50% across evaluated metrics.

1 Introduction

The sparse vector technique (SVT) Dwork et al. [2009, 2014] is one of the most fundamental algorithmic tools in DP, serving as a backbone for adaptive data analysis in many applications, such as feature selection Bassily et al. [2018], stream data analysis Hasidim et al. [2020], and top- c selection Lyu et al. [2017]. At a high level, SVT answers a sequence of queries on a given dataset and extracts useful information in a privacy-preserving manner. Unlike typical private query releases that directly reveal the noisy query results, *SVT discloses less information*—it outputs only a binary bit for each query, indicating whether the query result surpasses a predefined threshold (Cf. Figure 1). The major advantage of SVT over the typical private query releases is that only the positive queries (those whose results are above the predefined threshold) consume privacy, thus potentially allowing an infinite number of queries on a single dataset.

Despite the widespread usage of SVT, it still suffers from a low query accuracy Zhu and Wang [2020] due to a conservative privacy analysis, resulting in a sub-optimal noise selection. Specifically, prior works in the literature

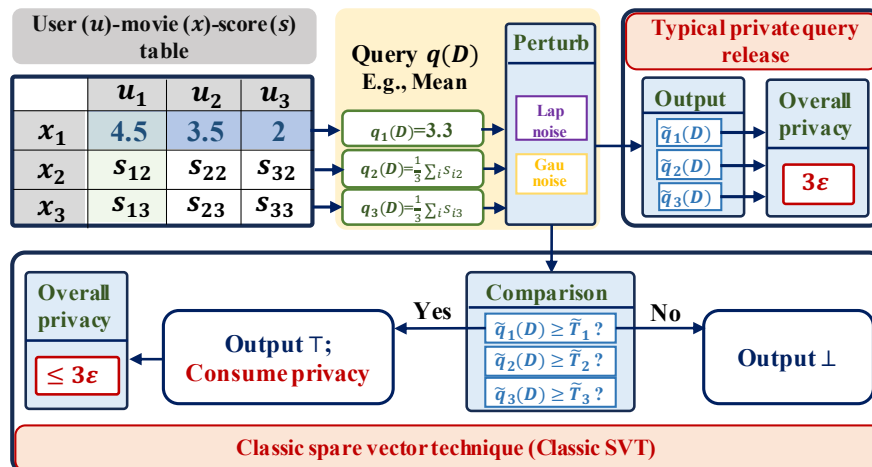


Figure 1: Classic sparse vector technique (SVT) and typical private query release on publicizing movies with the top-c highest scores. Classic SVT: after perturbing the movie score $q_i(D)$ and the predefined threshold T_i with either Laplacian or Gaussian noise, SVT compares the noisy score $\tilde{q}_i(D)$ and the noisy threshold \tilde{T}_i . If $\tilde{q}_i(D) \geq \tilde{T}_i$, \top is output. Otherwise, \perp is output. Typical private query releases: all \tilde{q}_i are released and sorted to obtain the noisy top-c movies.

naïvely approximate the privacy budget consumption of positive queries in SVT with that of differentially private query result releases (Cf. Section 2.2.1). However, since SVT discloses less information in each query (*i.e.*, only a binary bit instead of a noisy real-valued query result), this conservative privacy analysis approach overestimates its privacy risk. Consequently, SVT is constrained to use noise with large variance as in typical query releases for threshold and query perturbation, such as the Laplacian Lyu et al. [2017] or Gaussian Zhu and Wang [2020] noise. Such noise types then lead to an excessive noise injection and a sub-optimal query accuracy.

Motivated by this, our first contribution is providing a new privacy analysis (Cf. Theorem 2), which captures the *less informative nature of SVT* by precisely computing the privacy loss of the private comparison between thresholds and query results. Informally speaking, our analysis demonstrates that any noise whose cumulative distribution function satisfies the Lipschitz condition can be applied to SVT, allowing the use of noise types with smaller variance under the same privacy level. Based on our analysis, we identify the exponential noise, previously deemed non-applicable to SVT, as the optimal choice among all considered noise types. Exponential noise satisfies Theorem 2 tightly and benefits from a smaller variance compared to the others (Cf. Figure 4).

However, applying the exponential noise to SVT is challenging due to the bias introduced to the query results. The naïve bias correction method, which subtracts the expected value of random noise from the noisy query results, yields a sub-optimal performance. This is primarily because SVT requires correcting each noisy query result individually, whereas the naïve correction method is designed for correcting the aggregation of noisy query results Erlingsson et al. [2014]. When random noises are aggregated (as in the aggregation of noisy query results), their summed value approximates the expected value. In contrast, individual noisy query results are less concentrated around their expectations, resulting in less accurate corrections (Cf. Section 4.3.1).

To address this challenge, our second contribution involves developing an optimal threshold correction method¹ and an appending strategy, which effectively mitigate introduced bias and significantly enhance query accuracy. Instead of correcting the bias of each query result individually, our method focuses on optimizing the precision of the output binary bit vector. Specifically, we search for an optimal correction term that maximizes the probability of SVT distinguishing every true positive query from the true negative ones (Cf. Equation 8). Additionally, we introduce an appending strategy to complement the threshold correction method and boost the recall of SVT. Concretely, each query with a noisy negative output is appended to the end of the query queue for another round of querying. The intuition behind this is that, true positive queries are more likely to be identified as positive queries by SVT compared to the true negative ones after multiple rounds of querying, thus increasing the recall.

In conclusion, our main contributions are summarized as follows:

¹As we further discussed in Section 4.1, correcting the threshold is equivalent to correcting the noisy query results in SVT.

1. We provide a new privacy analysis that precisely captures the privacy loss of SVT. This analysis not only broadens the noise choices for query perturbation but also identifies exponential noise as the optimal choice among all considered ones.
2. Building on our privacy analysis, we propose a new SVT variant with exponential noise, where an optimal threshold correction method and an appending strategy are developed to mitigate the introduced bias and boost the query accuracy.
3. Comprehensive experiments conducted on both synthetic datasets and real-world datasets demonstrate that our proposed methods significantly increase the query accuracy of SVT by 2% \sim 50% across evaluated metrics.

2 Preliminaries

In this section, we first recall the definition (Cf. Definition 1), mechanisms (Cf. Equation 1), and properties of the differential privacy (*i.e.*, post-processing (Cf. Proposition 1) and composition (Cf. Theorem 1)). Then, we proceed to describe the sparse vector technique algorithm (Cf. Algorithm 1) and some of its predominant variants.

2.1 Differential Privacy

The differential privacy (DP) was first introduced by Dwork *et al.* Dwork [2006] and recently became a *de facto* standard for privacy protection. Roughly speaking, DP ensures that the likelihood of any specific output from a random algorithm varies little with sensitive neighboring inputs. The formal definition is as follows:

Definition 1 (Differential Privacy Dwork [2006]). *A randomized algorithm $\mathcal{M} : \mathbb{D} \rightarrow \mathbb{R}$ satisfies (ε, δ) -differential privacy if for any two neighboring datasets D and D' , and any output $o \subseteq \mathbb{O}$*

$$\Pr[\mathcal{M}(D) \in o] \leq e^\varepsilon \cdot \Pr[\mathcal{M}(D') \in o] + \delta.$$

When $\delta = 0$, we say that \mathcal{M} satisfies pure DP (denoted by ε -DP). Otherwise, it guarantees an approximate DP.

One of the typical methods of achieving DP is through the additive-noise mechanism, which corrupts and releases query results with additive noise randomly drawn from certain distributions Geng et al. [2019]. That is, given a dataset D , to guarantee DP, a randomized algorithm \mathcal{M} releases:

$$\mathcal{M}(D) = q(D) + X, \tag{1}$$

wherein $q(D)$ is the result of a query carried on D and X is the additive noise drawn from a probability distribution \mathcal{N} . The noise scale is calibrated to the sensitivity of $q(D)$ defined in the following:

Definition 2 (l_p -sensitivity). *For a real-valued query $q : \mathbb{D} \rightarrow \mathbb{R}$, the l_p -sensitivity of q is defined as:*

$$\Delta_p = \max_{D, D' \in \mathbb{D}} \|q(D) - q(D')\|_p,$$

where $\|\cdot\|_p$ denotes the l_p norm and D, D' is a pair of neighboring datasets that differ by one element.

The *Laplace mechanism* is one of the most classic additive-noise mechanisms that achieves ε -DP by letting X follow a Laplace distribution centered at 0 with a noise scale $b = \frac{\Delta_1}{\varepsilon}$, denoted as $X \sim \text{Lap}\left(\frac{\Delta_1}{\varepsilon}\right)$, where Δ_1 is the sensitivity of the query. Meanwhile, the *Gaussian mechanism* mechanism typically guarantees (ε, δ) -DP by drawing the noise X from a normal distribution $N(0, \sigma^2)$, where σ is proportional to $\frac{\Delta_2}{\varepsilon}$.

DP provides a rigorous privacy guarantee mathematically and is straightforward to achieve. Additionally, there are other two properties that contribute to the wide-ranging applications of DP. Firstly, it is immune to *post-processing*, which is formally described as follows:

Proposition 1 (Post-processing Dwork et al. [2014]). *Let $\mathcal{M} : \mathbb{D} \rightarrow \mathcal{R}$ be a randomized algorithm that is (ε, δ) differentially private. Let $f : \mathcal{R} \rightarrow \mathbb{R}$ be an arbitrary randomized mapping. Then $f \circ \mathcal{M}$ is (ε, δ) -differentially private.*

Secondly, different differentially private building blocks can be elegantly combined for designing more sophisticated algorithms, as described by the following theorem:

Theorem 1 (Sequential Composition Dwork [2006]). *Let $\mathcal{M}_i : \mathbb{N}^{|x|} \rightarrow \mathcal{R}_i$ be an $(\varepsilon_i, \delta_i)$ -differential privacy algorithm for $i \in [k]$. If $\mathcal{M}_k : \mathbb{N}^{|x|} \rightarrow \prod_{i=1}^k \mathcal{R}_i$ is defined to be $\mathcal{M}_{[k]}(x) = (\mathcal{M}_1(x), \dots, \mathcal{M}_k(x))$, then $\mathcal{M}_{[k]}$ is $(\sum_{i=1}^k \varepsilon_i, \sum_{i=1}^k \delta_i)$ -differentially private.*

Other composition theorems. In addition to sequential composition, more advanced composition theorems with tighter composition results are also utilized in the literature Dwork et al. [2010], Kairouz et al. [2015], Meiser and Mohammadi [2018], Zhu and Wang [2020], Gopi et al. [2021]. Among these, composition under *Rényi differential privacy* (RDP) Mironov [2017] is one of the widely adopted methods in the literature, owing to its concise and tight analysis result. RDP employs Rényi divergence as a tool for privacy measurement, and combining the RDP notion with Theorem 1 yields a tighter privacy bound. Zhu *et al.* Zhu and Wang [2020] later demonstrate that SVT can be combined with RDP for improved privacy guarantees. Although it is straightforward to extend the existing composition theorems applied to SVT to our proposed SVT variants Dwork et al. [2014], Zhu and Wang [2020], for ease of analysis, we derive our privacy analysis in this work based on Theorem 1. While we do not dive deep into the theoretical analysis of other composition theorems in this work, an empirical study on the performance of our proposed method under RDP composition is provided in Appendix I to offer further insights.

2.2 Sparse Vector Technique

Algorithm 1: SVT. Privately indicates if query results are above thresholds.

Input: $Q = \{q_1, q_2, \dots\}, \Delta, \varepsilon_1, \varepsilon_2, c, k_{max}, T = \{T_1, T_2, \dots\}$, option RESAMPLE

```

1  $\rho \sim \mathcal{N}_1(\varepsilon_1, \Delta); n_c = 0; n_a = 0;$ 
2 for  $i = 1, 2, 3, \dots, k_{max}$  do
3    $n_a = n_a + 1;$ 
4    $v_i \sim \mathcal{N}_2(\varepsilon_2, \Delta);$ 
5    $\tilde{q}_i(D) = q_i(D) + v_i;$  // Query perturbation
6    $\tilde{T}_i = T_i + \rho;$  // Threshold perturbation
7   if  $\tilde{q}_i(D) \geq \tilde{T}_i$  // Private comparison
8     then
9       Output  $a_i = \top;$ 
10       $n_c = n_c + 1;$ 
11      if RESAMPLE,  $\rho \sim \mathcal{N}_1(\varepsilon_1, \Delta);$ 
12      Abort if  $n_c \geq c$  or  $n_a \geq k_{max};$ 
13    else
14      Output  $a_i = \perp$ 
15    end
16 end
```

In principle, SVT works as follows. Given a sequence of queries $q_i(D)$ on a dataset D and their corresponding predefined thresholds T_i , SVT first perturbs them with random noise drawn from noise distribution \mathcal{N}_2 and \mathcal{N}_1 (Line 4, Line 5, Line 1, and Line 6), respectively. Then, it compares each noisy query result $\tilde{q}_i(D)$ with the noisy threshold \tilde{T}_i (Line 7). If $\tilde{q}_i(D)$ is no smaller than \tilde{T}_i , \top is output as a positive indicator (Line 9). Otherwise, \perp is output as a negative indicator (Line 14). The algorithm halts either when the number of positive outcomes reaches its maximum value c , or when the total number of queries exceeds its maximum value k_{max} (Line 12).

Different variants in the literature set this indicator to different values. For instance, Dwork et al. Dwork et al. [2009] set RESAMPLE to True, whereas Lyu et al. Lyu et al. [2017] argue that the overall privacy cost is significantly reduced by setting it to False, therefore significantly boosting the performance of SVT. Furthermore, Zhu et al. Zhu and Wang [2020] alternate True and False periodically for certain applications.

In this work, we provide a privacy analysis of our proposed method under both True and False settings (Cf. Theorem 3). As the empirical evaluation results for both settings demonstrate similar trends and RESAMPLE=True yields better performance in general Lyu et al. [2017], we only present the results of RESAMPLE set to True in Section 5.

2.2.1 Private Comparison

As mentioned above, to provide a rigorous DP guarantee, certain types of noise are required to ensure that for any noisy threshold \tilde{T}_i ,

$$\frac{\Pr[\tilde{q}_i(D) \geq \tilde{T}_i]}{\Pr[\tilde{q}_i(D') \geq \tilde{T}_i]} \leq e^\varepsilon \quad (2)$$

holds with high probability.

Previous works Dwork et al. [2009], Lyu et al. [2017], Zhu and Wang [2020] bound the probability ratio on the left of Inequality 2 by naïvely assuming that Inequality 2 is equivalent to the following:

$$\frac{\Pr[\tilde{q}_i(D) \in o]}{\Pr[\tilde{q}_i(D') \in o]} \leq e^\varepsilon, \quad (3)$$

where o is any possible output in the output space.

To ensure Inequality 3 hold, *Laplacian* ($Lap\left(\frac{\Delta f}{\varepsilon_{\varepsilon_1/\varepsilon_2}}\right)$) Dwork et al. [2009], Lyu et al. [2017] and *Gaussian* noise ($N(0, \sigma_{1/2})$), where σ_b for $b \in \{1, 2\}$ is a function of ε_b) Zhu and Wang [2020] are then adopted for both the query result and predefined threshold perturbation.

However, this privacy analysis overestimates the privacy risk in SVT, leading to an overly conservative choice of noise. Note that Inequality 2 is easier to achieve compared to Inequality 3: while Inequality 3 requires a rigorous bound on the probability ratio over every possible subset (o) in the output space, Inequality 3 splits the output space into two (*i.e.*, $\geq \tilde{T}_i$ and $< \tilde{T}_i$) and only requires a bound on the *accumulative* probability over the two parts. Thus, the high probability ratios (*i.e.*, the left side term in Inequality 3) incurred by some extreme subsets o in Inequality 3 are averaged down in Inequality 2 by those with relatively low probability ratios. In other words, let \mathcal{O}_i be the output space of $\tilde{q}_i(D)$, which is split into two parts: $\mathcal{R} := \{z \in \mathcal{O}_i | z \geq \tilde{T}_i\}$ and $\mathcal{L} := \mathcal{O}_i \setminus \mathcal{R}$. Then, by further splitting \mathcal{R} into n subsets that $\mathcal{R} = o_1 \cup \dots \cup o_n$, we have the following inequality holds:

$$\frac{\Pr[\tilde{q}_i(D) \geq \tilde{T}_i]}{\Pr[\tilde{q}_i(D') \geq \tilde{T}_i]} = \frac{\sum_{j=1}^n \Pr[\tilde{q}_i(D) \in o_j]}{\sum_{j=1}^n \Pr[\tilde{q}_i(D') \in o_j]} \leq \max_{j \in [n]} \frac{\Pr[\tilde{q}_i(D) \in o_j]}{\Pr[\tilde{q}_i(D') \in o_j]}$$

Intuitively, there may be some noise distributions that, although they do not satisfy Inequality 3, can still ensure that Inequality 2 holds with high probability while introducing less distortion.

2.2.2 Advantage of SVT Over Typical Private Releases

One of the most unique properties of SVT, as well as its variants, is that only the positive outcomes incur privacy costs. Specifically, the overall privacy budget ε is independent of the value of k_{max} depends instead on the noise scale (*i.e.*, the variance of the noise) of each noisy query and the number of positive outcomes n_c .

Example. Consider a scenario where a data analyst wants to identify the top- c most popular movies (Cf. Figure 1). Each movie is rated by a group of individuals who have watched it. Directly releasing the score of each movie (*i.e.*, $q_i(D)$ in Figure 1) may reveal sensitive information about whether an individual has watched a particular movie, thus necessitating the use of DP to protect individual privacy. *Typical private query releases* perturb and release the score of all candidate movies, which incurs a privacy budget proportional to the number of all candidates n . In contrast, using SVT to approximate the top- c movies by only outputting the indices of first c films whose scores exceed a predefined threshold T results in an overall privacy cost proportional to c rather than n . When $c \ll n$, this approach significantly reduces the privacy cost.

Note that Figure 1 uses $\text{MEAN}(D)$ as an example of query $q_i(D)$. In practice, $q_i(D)$ can represent any queries with real-valued answers, such as $\text{SUM}(D)$, $\text{COUNT}(D)$, $\text{MAX}(D)$. Furthermore, while we use top- c selection to demonstrate the effectiveness of our proposed method, SVT can be applied to many other scenarios where queries need to be evaluated against specific criteria (predefined threshold) in a privacy-preserving manner, such as feature selection Bassily et al. [2018], steaming data analysis Hasidim et al. [2020].

2.2.3 Utility Metric

The utility of SVT is measured by a specialized utility metric, namely (α, β) -accuracy Dwork et al. [2014].

Definition 3 ((α, β) -accuracy). *An algorithm which outputs a stream of answers $a_1, \dots, \in \{\top, \perp\}^*$ in response to a stream of k queries q_1, \dots, q_k is (α, β) -accurate with respect to a threshold T if except with probability at most β , the algorithm does not halt before q_k , and for all $a_i = \top$:*

$$q_i(D) \geq T - \alpha$$

and for all $a_i = \perp$:

$$q_i(D) \leq T + \alpha.$$

Definition 3 specifies that given an error tolerance parameter α , SVT achieves a success probability of at least $1 - \beta$. Particularly, queries with results falling within the interval $[T - \alpha, T + \alpha]$ are allowed to be misclassified. For instance,

if a query $q(D)$ falls within $(T, T + \alpha]$, the SVT algorithm is still considered successful even if it incorrectly classifies $q(D)$ as negative by outputting \perp . Specifically, it is demonstrated by prior works that the SVT algorithm, when using Laplacian noise (*i.e.*, \mathcal{N}_1 and \mathcal{N}_2 are Laplace distributions), is $(\frac{8(\ln k + \ln \frac{2}{\beta})}{\epsilon}, \beta)$ -accurate Dwork et al. [2014].

3 Privacy Analysis Revisit

As discussed in Section 2.2.1, it has been observed that previous privacy proofs tend to overestimate the privacy risk in SVT by bounding the privacy over all possible subsets in the output space of query results. The underlying assumption is that disclosing a binary bit is as risky as directly revealing the query result itself. However, this may not hold true: intuitively, a binary bit leaks less information than the complete query result and, therefore, should pose a lower risk.

Motivated by this, we revisit the privacy analysis of SVT, taking into account its less informative nature. We provide a new analysis result in Theorem 2. Informally speaking, our results indicate that for query perturbation, SVT poses a less stringent constraint on eligible noise distributions compared to typical private query releases, thereby accommodating a broader range of noise distributions.

Theorem 2 (Privacy of SVT). *Algorithm 1 satisfies differential privacy if for any real numbers b_1, b_2 , there are two positive real numbers k_1 and k_2 such that the following inequalities hold:*

$$|\ln(f_1(x)) - \ln(f_1(x + b_1))| \leq k_1|b_1|, \quad (4)$$

$$|\ln(1 - F_2(x)) - \ln(1 - F_2(x + b_2))| \leq k_2|b_2|, \quad (5)$$

where $f_1(\cdot)$ and $F_2(\cdot)$ are the probability density function of \mathcal{N}_1 and the cumulative function of the \mathcal{N}_2 , respectively.

We defer the proof of Theorem 2 to Appendix A and provide only the key takeaways here.

Takeaways from Theorem 2. First, Theorem 2 *broadens* the range of noise distributions for query perturbation. Specifically, as indicated by Equation 11, distributions such as the exponential and Gumbel distribution are now eligible for query perturbation (*i.e.*, \mathcal{N}_2 in Algorithm 1), whereas these types of noise were previously considered unsuitable for SVT. Second, although Theorem 2 relaxes the constraints on noise distributions for *query result perturbation*, the eligible noise distributions for *threshold perturbation* (*i.e.*, \mathcal{N}_1 in Algorithm 1) remain *unchanged* compared to the previous work. This is because, despite the query results not being directly released, the predefined threshold is public information. To prevent negative queries from consuming privacy, the true threshold value, which is compared with the noisy query result, must also be obscured. Hence, the same noise distributions, such as Laplacian or Gaussian, are used in traditional private query releases.

To clarify, we summarize some of the most commonly used noise distributions for both threshold perturbation and query result perturbation in Table 1.

Table 1: Feasible noise distributions for SVT

	Laplace	Gaussian	Exponential	Gumbel
Query Result	✓	✓	✓	✓
Threshold	✓	✓	×	×

4 Construction

Based on the two crucial takeaways discussed in Section 3, we propose an enhanced SVT algorithm with improved query accuracy, referred to as SVT-Exp. This algorithm is summarized in Algorithm 2, with key changes in the algorithm design highlighted by underlines. Additionally, the main steps of Algorithm 2 are illustrated in Figure 2 for better understanding.

4.1 Overview

In summary, our proposed enhanced SVT algorithm introduces three key improvements:

① ① **The algorithm uses exponential noise for query perturbation** (Line 6). This choice is based on the fact that the cumulative probability function of exponential noise tightly satisfies Equation 11 in Theorem 2. Meanwhile, it

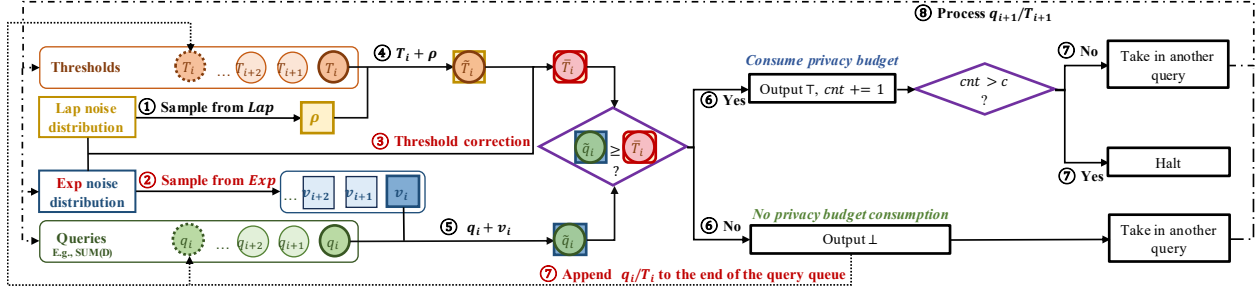


Figure 2: The overall design of Algorithm 2, with our newly proposed methods in this work emphasized with red color. The RESAMPLE is set to False. In step ③, the optimal threshold correction term r^{op} is computed based on the Laplace and exponential distribution and added to the current threshold. The threshold (step ④) and the query (step ⑤) are then perturbed with random noise sampled in step ① and ②, respectively. After comparing the noisy threshold with the noisy query in step ⑥, the algorithm outputs \top and compares the number of accumulated positive outcomes (cnt) with a positive threshold c if $\tilde{q}_i \geq \tilde{T}_i$. Otherwise, \perp is output. If APPEND is set to True, the negative query is appended to the end of the query queue for an additional round of querying. If the algorithm does not halt in step ⑦, it takes in another threshold-query pair and repeats the procedure (step ⑧).

Algorithm 2: SVT with exponential noise, optimal threshold correction, and appending strategy (SVT-Exp).

Input: $Q = \{q_1, q_2, \dots\}, \Delta, \varepsilon_1, \varepsilon_2, \lambda, c, k_{max}, T = \{T_1, T_2, \dots\}, \alpha, \varepsilon, m, e, k$ option RESAMPLE, option APPEND.

```

1  $\varepsilon = \varepsilon_1 + \varepsilon_2; n_c = 0; n_a = 0;$ 
2  $b = \frac{\Delta}{\varepsilon_1}; \rho \sim Lap(b);$ 
3  $r^{op} = \text{CorrectionTerm}(b, \lambda, \alpha, m, e, k);$  // Threshold correction term computation
4 for  $i = 1, 2, 3, \dots$  do
5    $n_a = n_a + 1;$ 
6    $\lambda = \frac{\varepsilon_2}{2c\Delta}; v_i \sim Exp(\frac{1}{\lambda});$  // Query perturbation
7    $\tilde{q}_i(D) = q_i(D) + v_i;$ 
8    $\tilde{T}_i = T_i + \rho;$  // Threshold perturbation
9   if  $\tilde{q}_i(D) \geq \tilde{T}_i + r^{op}$  // Private comparison
10  then
11    Output  $a_i = \top;$ 
12     $n_c = n_c + 1;$ 
13     $S_\top = S_\top \cup i;$ 
14    if RESAMPLE,  $\rho \sim Lap(b);$ 
15    Abort if  $n_c \geq c$  or  $n_a \geq k_{max};$ 
16  else
17    Output  $a_i = \perp;$ 
18    if APPEND then
19       $Q = Q \cup \{q_i\}; T = T \cup \{T_i\};$  // Appending queries with noisy negative outcomes
20    end
21  end
22 end

```

exhibits a much smaller variance compared to other noise distributions considered, resulting in less data distortion and enhanced query accuracy.

②: An optimal threshold correction term is computed by maximizing the (α, β) -accuracy of the SVT with exponential noise (Line 3), and added to the noisy thresholds \tilde{T}_i (Line 9). Correcting the threshold is crucial when using exponential noise (or other noise distributions centered at non-zero values) as it introduces bias into the query

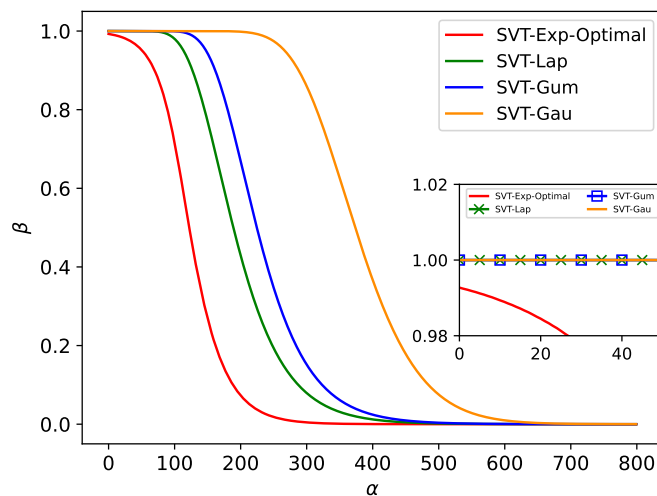


Figure 3: The (α, β) -accuracy of SVT algorithms with four different types of noise: the SVT with the exponential noise and the optimal threshold correction; SVT with the Laplacian noise; SVT with the Gumbel noise and the mean threshold correction; and SVT with Gaussian noise. Parameter k in Theorem 4 is set to 50 and the overall privacy budget $\varepsilon = 1$.

results². Intuitively, the correction term that maximizes the (α, β) -accuracy ensures the highest success probability (*i.e.*, $1 - \beta$) for SVT, thereby improving query accuracy.

③: **An appending strategy has been developed**, where noisy negative queries (*i.e.*, $q_i(D)$ for $\tilde{q}_i(D) < \tilde{T}_i(D)$) are appended to the query queue for an additional round of querying (Line 18 to Line 19). Generally speaking, while our optimal threshold correction method effectively increases the precision of SVT, the appending strategy further increases its recall. The rationale behind this strategy is that for a positive query where $q_i(D) \geq \tilde{T}_i$, comparing the noisy threshold \tilde{T}_i with $\tilde{q}_i(D)$ multiple times increases the likelihood of $q_i(D)$ identified as a positive query.

The concrete details of our developed methods and strategy are presented in Section 4.2, Section 4.3, and Section 4.4. Additionally, the privacy guarantee and the utility guarantee of Algorithm 2 are provided in Theorem 3 and Theorem 4, respectively. The proof of these theorems is deferred to Appendix B and Appendix C.

Theorem 3 (Privacy guarantee). *Let c denote the number of positive outcomes output by Algorithm 2. Algorithm 2 satisfies $(\varepsilon_1 + \varepsilon_2)$ -differential privacy when `RESAMPLE` is set to `False`, and $(c\varepsilon_1, \varepsilon_2)$ -differential privacy when `RESAMPLE` is set to `True`, where ε_1 and ε_2 are the privacy budgets for threshold and query perturbation, respectively.*

For the utility guarantee, following the convention Dwork et al. [2014], Lyu et al. [2017], (α, β) -accuracy is adopted as the utility metric. The parameters in Algorithm 2 are set as $\Delta = 1$, $\varepsilon_1 = \varepsilon_2 = \frac{\varepsilon}{2}$ and $c = 1$ for ease of computation and comparison. As demonstrated in Theorem 4, compared to SVT algorithms where the Laplacian noise is adopted for query perturbation, Algorithm 2 demonstrates a clear advantage.

Theorem 4 (Utility guarantee). *Given any k records such that $|\{i < k : d_i \geq t - \alpha\}| = 0$ (*i.e.*, the record above and closest to the threshold is the last one), Algorithm 2 is at least $(\frac{4(\ln k + \ln \frac{2}{\beta})}{\varepsilon}, \beta)$ -accurate.*

Additionally, note that the assumptions made on parameter settings in Theorem 4 may not fully align with real-world scenarios. Therefore, we further provide a numerical utility analysis under a more practical setting in Figure 3, which shows that the value of β of Algorithm 2 is consistently below that of other baselines for a fixed α , further demonstrating the effectiveness of our method.

4.2 Query Perturbation with Exponential Noise

In this section, we justify the use of exponential noise in Algorithm 2 for the following two reasons:

²Note that correcting the threshold is equivalent to correcting the query results. In essence, as SVT compares $\tilde{q}_i - \tilde{T}_i$ with 0. Therefore, adding the correction term to the predefined threshold \tilde{T}_i is the same as subtracting it from the query result $\tilde{q}_i(D)$.

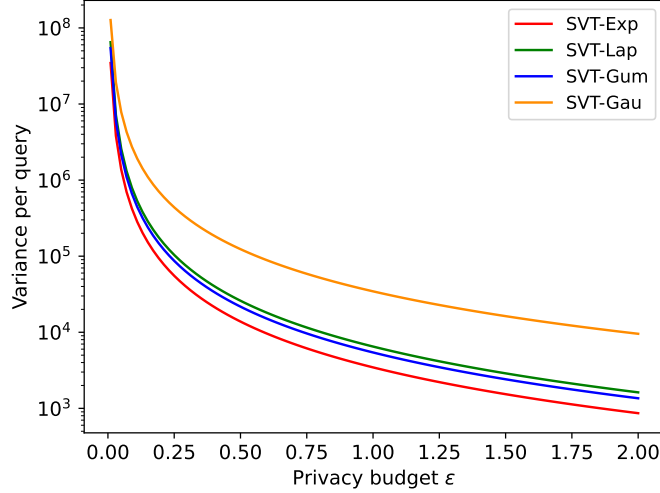


Figure 4: The variance of SVT with four different types of noise (*i.e.*, exponential noise, Laplacian noise, Gumbel noise, and Gaussian noise). The privacy budget ϵ varies from 0.01 to 2. c is set to 50. The y-axis is log-based. Note that the threshold correction does not affect the query variance.

First, exponential noise guarantees DP for SVT, as its cumulative function,

$$F(x; \lambda) = \begin{cases} 1 - \exp(-\lambda x) & x \geq 0 \\ 0 & x < 0 \end{cases},$$

tightly satisfies Equation 11 with $k_2 = \lambda$ for any $\lambda > 0$. However, note that the exponential distribution does not satisfy Equation 10, and therefore cannot be used for threshold perturbation. Since the Laplace distribution is one of the most commonly and frequently adopted noise distributions in SVT, we use it to perturb the predefined threshold, following convention.

Second, exponential noise yields the smallest variance on the private comparison result (*i.e.*, $\tilde{q}_i(D) \geq \tilde{T}_i + r^{op}$) in Algorithm 2 among all evaluated noises, yielding the least data distortion among all compared methods. Specifically, as also stated in Lyu et al. [2017], the variance of the private comparison result V is written as follows:

$$V = \text{Var} \left(\text{Lap} \left(\frac{\Delta}{\varepsilon_1} \right) \right) + \text{Var} \left(\text{Exp} \left(\frac{2c\Delta}{\varepsilon_2} \right) \right). \quad (6)$$

A smaller V indicates a smaller data distortion, thus a potentially higher query accuracy. Given an overall privacy budget ε , by varying w such that $\varepsilon_2 = w\varepsilon_1$ and $\varepsilon = \varepsilon_1 + \varepsilon_2$, V can be minimized for any fixed pair of noise distributions Lyu et al. [2017] (Cf. Appendix G). As shown in Figure 4 where the minimal V for different \mathcal{N}_2 in Algorithm 2 are depicted, exponential distribution yields the smallest private comparison variance.

4.3 Optimal Threshold Correction

In this section, we elaborate on our optimal threshold correction by: (1) providing the motivations necessitating our design (Cf. Section 4.3.1); (2) detailing our correction methodology, which incorporates derivation of the success probability of SVT and computation of the optimal correction term (Cf. Section 4.3.2); and (3) presenting a numerical computation framework that generalizes our correction method to broader applications (Cf. Section 4.3.3).

4.3.1 Motivations.

Though the exponential noise demonstrates properties that can theoretically boost query accuracy, applying it to SVT is challenging due to the introduced bias. Specifically, the expectation of the difference between a noisy query and its corresponding noisy threshold is written as follows:

$$E \left(\tilde{q}_i(D) - \tilde{T}_i \right) = q_i(D) - T_i + \frac{2c\Delta}{\varepsilon_2}.$$

Due to the introduction of a positive bias $\frac{2c\Delta}{\varepsilon_2}$, the algorithm is likely to mistakenly classify queries $q_i(D)$ as positives if they fall within the range $T_i \geq q_i(D) \geq T_i - \frac{2c\Delta}{\varepsilon_2}$. As a result, the query accuracy is compromised for two reasons. First, as mentioned above, the false positive rate increases. Second, as described in Algorithm 2, to limit the overall privacy budget consumption, no more than c records are allowed to be identified as positive queries. Since the false positive queries occupy these c spots, the subsequent true positive queries are unable to be output, thereby decreasing the precision.

A naïve solution is to directly subtract the bias from each $q_i(D)$ or add the bias to each T_i Wang et al. [2017], Ye et al. [2019], Liu et al. [2022, 2023]. However, this method yields a sub-optimal performance when applied to SVT. The primary reason is that this approach is designed for correcting the aggregation of n noisy query results, whereas our focus is on correcting each noisy query result individually. According to the law of large numbers, the mean of the aggregation with larger n tends to converge to its expectation. That is to say, as n increases, the mean of the aggregated results approaches the noise expectation more closely. Consequently, correcting the aggregate of noisy query results by subtracting the expectation often achieves satisfactory accuracy. However, since our approach targets individual noisy results (*i.e.*, $n = 1$), this method does not provide the same level of performance in SVT as it does with aggregated noisy queries.

4.3.2 Methodology.

Motivated by this, we have developed a new correction method that focuses on improving the precision of the output binary vector rather than correcting each individual query result. At a high level, inspired by the definition of (α, β) -accuracy (Cf. Definition 3), we compute the success probability of the SVT algorithm by multiplying the probability of each query being corrected classified. We then derive an optimal threshold correction term by maximizing this success probability. In essence, our optimal correction method increases the threshold value to enhance the precision of SVT, which is further elucidated in the analysis presented in Figure 5.

Success probability of SVT. We begin by considering a simple case where $c = 1$. Assume there are k true negative queries before the true positive query. Given a fixed error tolerance parameter α , the success probability of Algorithm 2 with a threshold correction term r is defined as follows:

$$p(r) = \prod_{i=1}^k \Pr \left[\tilde{q}_i(D) - \alpha < \tilde{T}_i + r \right] \cdot \Pr \left[\tilde{q}_j(D) + \alpha \geq \tilde{T}_j + r \right], \quad (7)$$

where $\tilde{q}_{i/j}(D) = q_{i/j}(D) + \text{Exp}(\frac{1}{\lambda})$, and $\tilde{T}_{i/j} = T_{i/j} + \text{Lap}(b)$. Note that here we abuse the notion $\text{Exp}(\cdot)$ and $\text{Lap}(\cdot)$ to denote the random variables drawn from exponential distribution and Laplace distribution, respectively.

Takeaways from Equation 7. First, Equation 7 is directly related to the (α, β) -accuracy. Specifically, for a fixed α , the value of β with a threshold correction term r is given by $1 - p(r)$. Second, by maximizing $p(r)$, we maximize the query accuracy of SVT, which in turn improves empirical performance. Third, Equation 7 can be easily extended to scenarios where $c > 1$ by: ① dividing all queries into subroutines, each containing exactly one positive query; and ② multiplying the success probability of each subroutine.

However, Equation 7 cannot be directly adopted as it is data-dependent, which could lead to privacy leakage. To address this issue, we adopt a worst-case assumption by setting $q_{i/j}(D) = T_{i/j}$. Thus, the success probability $p(r)$ can be expressed as:

$$p(r) = (\Gamma(r + \alpha))^k \cdot (1 - \Gamma(r - \alpha)), \quad (8)$$

where $\Gamma(\cdot)$ is the cumulative distribution function (CDF) of the random variable $Z = X - Y$. Here X and Y are random variables drawn from distribution $\text{Exp}(\frac{1}{\lambda})$ and $\text{Lap}(b)$, respectively. The shape of the probability density function (PDF) of Z is illustrated in Figure 5(a), and the explicit expression of $p(r)$ is detailed in Appendix D.

Optimal correction term. After demonstrating that the maximum value of $p(r)$ exists (Cf. Appendix E), the optimal threshold correction is obtained by:

$$r^{op} = \arg \max p(r). \quad (9)$$

To offer a better understanding, we perform a detailed analysis of Equation 8 and Equation 9 (Cf. Figure 5), and the key findings are summarized as follows:

First, as shown in Figure 5(b), an increasing number of negative queries (k) leads to a larger threshold correction term (r^{op}). As k grows, SVT is more likely to halt before the last true positive query, which is referred to as ‘early halting’. Consequently, a larger correction term is necessary to mitigate early halting, thereby enhancing the precision of the SVT algorithm.

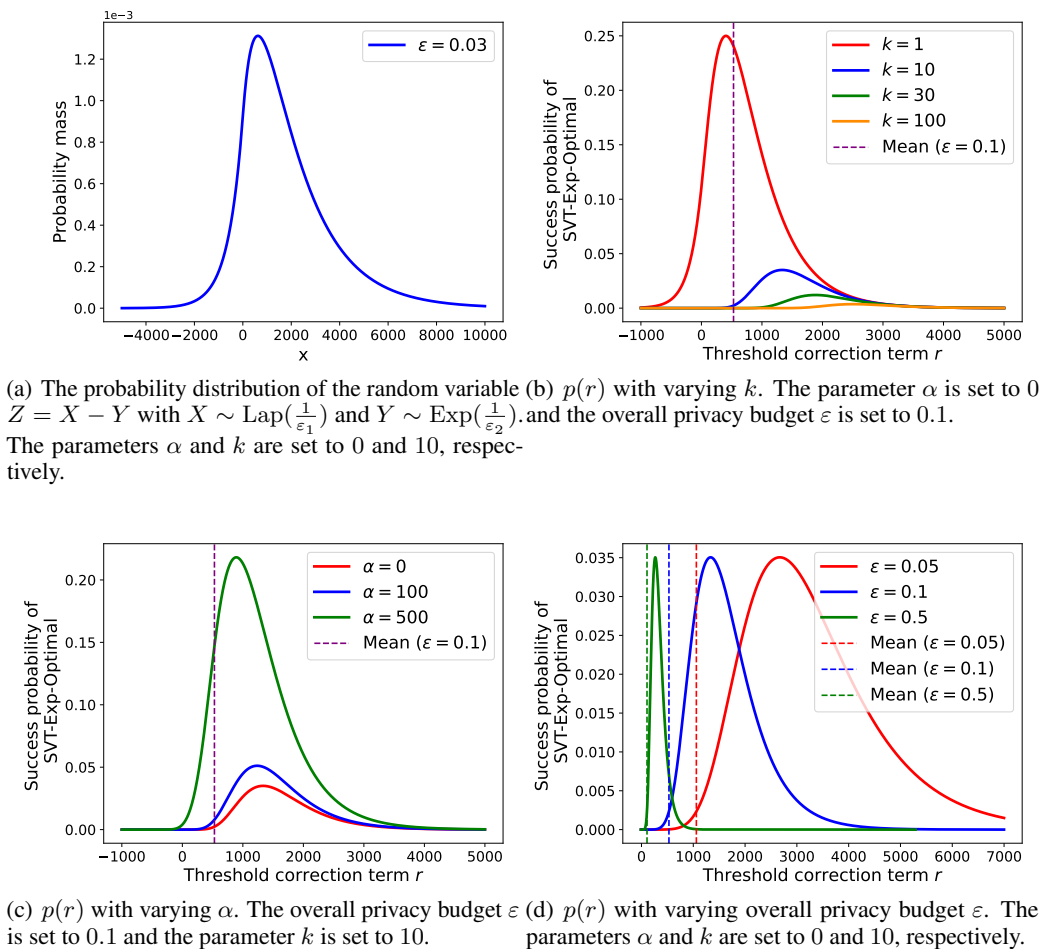


Figure 5: The numerical analysis of Equation 8. Dashed lines are the mean of the exponential noise distribution. Each privacy ϵ has a corresponding mean.

Second, as shown in Figure 5(c), an increase in the error tolerance parameter α results in a higher success probability and a smaller threshold correction term r^{op} . The rationale is that a larger α allows more false negative or false positive queries during the query process. Consequently, a smaller threshold correction term is sufficient to achieve a high success probability. Note that α is a hyperparameter chosen by the data analysts. For generality, this work defaults to $\alpha = 0$, irrespective of specific data distributions.

Third, as shown in Figure 5(d), an increase in the privacy budget results in a smaller threshold correction term. This is because a larger privacy budget leads to lower noise variances, which reduces data distortion and results in noisy query results that are more tightly concentrated around their expectations. Consequently, a smaller threshold correction term is adequate to prevent the early-halting issue and achieve an optimal success probability.

4.3.3 Numerical Computation Framework.

To improve the scalability of the optimal threshold correction method, we further propose a numerical computation framework, which is summarized in Algorithm 3 and Algorithm 4. Instead of deriving the analytical formula for $\Gamma(\cdot)$ in Equation 8, we first discretize the noise distributions \mathcal{N}_1 and \mathcal{N}_2 used in Algorithm 2. We then convolve these discretized distributions using the Fast Fourier Transform (FFT) to obtain the numerical representation of Γ . The optimal threshold correction term, \bar{r}^{op} , is determined by maximizing $\bar{p}(r)$, which is calculated based on this numerical $\Gamma(\cdot)$. Hereinafter, we use the combination of Laplace and exponential distributions as an example to illustrate the concrete steps of our framework. First, to convert the continuous noise distributions into discretized sequences, we define a boundary B within which most of the probability mass (e.g., $1 - e$ as indicated in Line 1 of Algorithm 3) is concentrated. Next, in Algorithm 4, we discretize the event space within B into u chunks, with each chunk having a

Algorithm 3: CorrectionTerm: Numerical threshold correction.

Input: $b, \lambda, \alpha, m, e, k$

- 1 $B = F_{Exp}^{-1}(1 - e); //$ Boundary
- 2 $\bar{L} = \text{Discretizer}(Lap(b), m, B); //$ Discretize Laplace distribution
- 3 $\bar{E} = \text{Discretizer}(Exp(\frac{1}{\lambda}), m, B); //$ Discretize exponential distribution
- 4 $\bar{\Gamma} = \text{CONVOLVE}(\bar{L}, \bar{E}); //$ Convolution with FFT
- 5 Compute \bar{r}^{op} that maximize $(\bar{\Gamma}(\bar{r} + \alpha))^k \cdot (1 - \bar{\Gamma}(\bar{r} - \alpha));$
- 6 **return** $\bar{r}^{op};$

Algorithm 4: Discretizer

Input: CDF, m, B

- 1 $u = \frac{B}{m-1};$
- 2 **for** $i=-m+1$ to $m-2$ **do**
- 3 | $h_i = \text{CDF}((i+1) \cdot u) - \text{CDF}(i \cdot u);$
- 4 **end**
- 5 $h_{-\infty} = \text{CDF}((1-m) \cdot u);$
- 6 $h_{+\infty} = 1 - \text{CDF}(m-1 \cdot u);$
- 7 $\bar{D} = \{h_{-\infty}, h_i \text{ for } i \text{ in } (-m, m) \cap \mathbb{Z}, h_{+\infty}\};$
- 8 **return** $\bar{D};$

mesh size m (Line 1). The events in each chunk are aggregated into a new event with a probability mass h_i (Line 3). Additionally, the probability mass of events exceeding B is assigned to the positive infinity bracket, while events below $-B$ are placed in the negative infinity bracket (Lines 5 and Line 6 in Algorithm 4). Subsequently, we use Fast Fourier Transform (FFT) Nussbaumer and Nussbaumer [1982] to compute the discretized distribution $\bar{\Gamma}$ by convolving the discretized Laplace distribution \bar{L} and the discretized exponential distribution \bar{E} , where we define that $\infty + x = \infty$ for any $x \in \mathbb{R}$. Finally, the correction term \bar{r} is determined using $\bar{\Gamma}$ based on Equation 9.

The primary advantage of this numerical computation framework is its strong scalability to various types of noise distributions. While we can derive the explicit formula for $\Gamma(\cdot)$ when using Laplace and exponential distributions for query and threshold perturbation, respectively (Cf. Appendix D), deriving such formulas becomes complex when combining other distributions, such as Gaussian and exponential. This numerical framework allows privacy practitioners to apply the optimal threshold correction method to any noise distributions. It is important to note that our numerical framework may introduce additional computation costs due to the discretization and convolution steps. To provide further insights, we analyze the trade-off between the running time of our algorithm and the estimation accuracy of $\bar{p}(r)$ and \bar{r}^{op} in Appendix K. In summary, our analysis demonstrates that the proposed method can achieve highly accurate estimations with minimal additional computation cost.

4.4 Appending Strategy

As discussed earlier, our threshold correction method enhances the performance of SVT by increasing the value of the threshold, which in turn improves the precision of the algorithm. However, a higher threshold can also result in a reduced recall. This occurs because true positive queries with relatively small results are less likely to exceed the adjusted threshold.

To further enhance recall, we propose an appending strategy. As shown in Figure 2 Step ⑦ and Algorithm 2 from Line 18 to Line 19, each query identified as negative by the algorithm is appended to the end of the query queue for another round of querying. In settings where there is an infinite number of queries (e.g., streaming data analysis, where new data and queries continuously arrive), these queries may be randomly inserted back into the queue.

The rationale behind this strategy is twofold. First, as stated in Theorem 3, re-querying the outputs identified as negative incurs no additional privacy cost. Second, conducting multiple rounds of querying increases the likelihood of correctly identifying true positive queries that were misclassified initially. Simultaneously, it also enlarges the probability gap between positive queries correctly identified as positive and negative queries mistakenly classified as positive. Concretely, for each query $q_i(D)$, the probability of it identified as positive in each round is

$$p_i = \Pr[q_i(D) + \text{Exp}(\frac{1}{\lambda}) \geq T_i + r + \text{Lap}(b)].$$

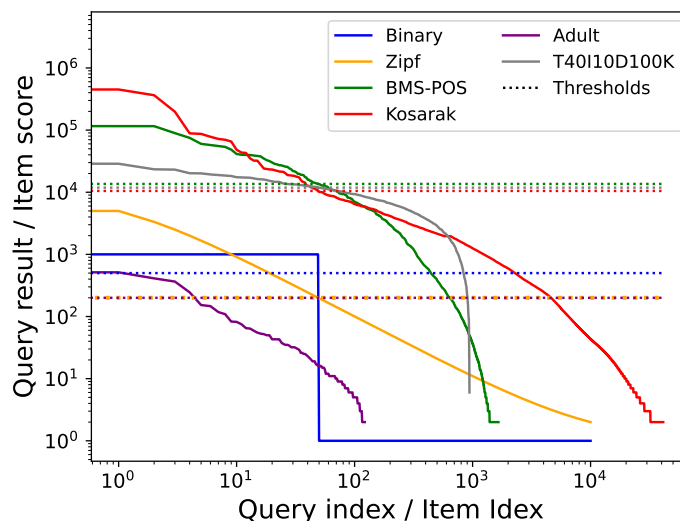


Figure 6: The scores of items of 6 datasets. All the items are in descending order based on their scores, which are plotted in a log-based manner for clarity. Dashed lines in Corresponding colors are the predefined thresholds we adopt in this work.

After t rounds of querying, this probability increases to tp_i . Also note that the larger the difference $q_i(D) - T_i$, the higher the p_i . Therefore, after multiple rounds, the probability of $q_i(D)$ being identified as positive is $t(p_i - p_j)$ higher than for $q_j(D)$, where $q_i(D) - T_i \geq q_j(D) - T_j$.

5 Evaluation

Before presenting our main results in Section 5.5, we detail the used datasets in Section 5.1, the adopted utility metrics in Section 5.2, the compared baselines in Section 5.3, and the selected parameters for our experiments in Section 5.4.

5.1 Datasets and Implementations

This work uses six different datasets: three real-world and three synthetic. Detailed information is provided in Table 2.

Table 2: Dataset details. # · denotes the number of ·, and the ‘Threshold’ is the predefined threshold we use in SVT for each dataset.

	# of records	# of items	Threshold	Type
Binary	-	10,000	500	synthetic
Zipf	-	10,000	200	
T40I10D100K Shakeri and Pedram [2012]	100,000	942	11,850	real-world
BMS-POS Zheng et al. [2001]	515,597	1,657	13,600	
Kosarak Aggarwal et al. [2009]	990,002	41,270	10,500	
Adult Becker and Kohavi [1996]	48,843	123	200	

For the real-world datasets and the T40I10D100K dataset, each item’s score is based on its frequency across records. Specifically, for each item I_i in the dataset, the score $s_i = \sum_{j=1}^n \mathbb{1}(I_j^i = 1)$, where I_j^i is an indicator of whether the record R_j contains item I_i , and n is the total number of records. For the remaining synthetic datasets, scores are assigned directly. In the Binary dataset, each positive query is assigned a score of 1,000, while negative queries receive a score of 0. In the Zipf dataset, each item’s score is proportional to $\frac{1}{i}$, with the score calculated as $s_i = \frac{1}{i} \times 10,000$. We use m to denote the total number of items. Additionally, Figure 6 plots the item scores for each dataset for further insights.

All experiments are conducted on a laptop (6-core Intel Core i7 CPU at 2.2 GHz with 16-GB RAM).

5.2 Queries and Utility Metric

5.2.1 Queries

The effectiveness of our proposed method is general but is validated here within the top- c selection problem, a common application for SVT Lyu et al. [2017], Zhu and Wang [2020]. In this scenario, we use SVT to approximately query items with the top- c highest scores in each dataset.

Specifically, we first shuffle the items randomly, then query each item’s score (*i.e.*, $q_i(D) = s_i$) and compare it to the threshold T . If $q_i(D) \geq T$, the corresponding query index i is output. The algorithm halts either when c indices is output or the number of queries reaches a maximum limit k_{max} . The choice of T is crucial for query accuracy, but determining an appropriate threshold is beyond this work’s scope. Various methods for threshold determination are discussed in the literature Lee and Clifton [2014], Carvalho et al. [2020].

5.2.2 Utility Metrics

We evaluate SVT’s performance on the top- c selection problem using two primary metrics: **F1-score** Fawcett [2006] and normalized cumulative rank (NCR). The F1-score is computed as:

$$F1 = \frac{2 \cdot \text{precision} \cdot \text{recall}}{\text{precision} + \text{recall}} = \frac{2TP}{2TP + FP + FN},$$

where TP is the number of true positive queries, FP is the number of false positive queries, and FN is the number of false negative queries. However, the F1-score is more suited for unordered settings, where missing a top result incurs the same penalty as missing a lower-ranked result Lyu et al. [2017]. To address this, we also use the Normalized Cumulative Rank (NCR) Lyu et al. [2017]. In NCR, each query q_i is assigned a rank score defined as follows: the top query (*i.e.*, top-1) receives a score of c , the next receives $c - 1$, and so on Lyu et al. [2017]. Queries below the threshold receive a score of 0. The total score for positive outcomes is then normalized to the range $[0, 1]$ by dividing by $\frac{c(c+1)}{2}$, the maximum possible score. Since the results for the F1-score demonstrate similar trends as NCR, detailed F1-score results are provided in Appendix H.

5.3 Baselines

Table 3 lists all the methods compared in this work. We evaluate our method, which uses exponential noise for query perturbation, against **SVT-Lap** Lyu et al. [2017], **SVT-Gau** Zhu and Wang [2020], and **SVT-Gum**. While SVT-Lap and SVT-Gau are two of the most frequently used SVT variants in the literature, SVT-Gum is a new variant proposed in this work. SVT-Gum meets the constraints in Theorem 2 but has a slightly larger variance compared to SVT-Exp. More details about SVT-Gum are provided in Appendix F. Additionally, to provide more insights, we also compare our method with the ‘upper bound’ of query accuracy, which is obtained by directly ranking the noisy query results perturbed with random noise drawn from $\text{Exp}\left(\frac{\Delta}{\varepsilon_2}\right)$. Regarding threshold correction, we compare SVT-Exp with optimal threshold correction to SVT-Exp with no threshold correction and to SVT-Exp with mean correction (*i.e.*, the naïve solution in Section 4.3.1).

Table 3: Baseline methods. Lap, Exp, Gau, and Gum refer to Laplace, exponential, Gaussian, and Gumbel distribution, respectively. ‘Optimal’ represents our optimal threshold correction method, while ‘Mean’ represents the naïve correction method by subtracting the mean of the noise.

	Noise for query	Noise for threshold	Threshold correction
SVT-Exp upper bound	-	Exp	-
SVT-Exp (optimal) (Alg. 2)	Lap	Exp	Optimal
SVT-Exp (mean)	Lap	Exp	Mean
SVT-Exp (no)	Lap	Exp	No
SVT-Gumbel	Lap	Gum	Mean
SVT-Lap	Lap	Lap	No
SVT-Gau	Gau	Gau	No

5.4 Parameter Selection

This work involves several privacy parameters: the failure rate δ , the overall privacy budget ε , the privacy budget for threshold perturbation (*i.e.*, ε_1), and the privacy budget for query perturbation (*i.e.*, ε_2). For SVT-Gau, δ is set to $\frac{1}{n}$,

following convention Dwork et al. [2014], Liu et al. [2022], while in other settings, δ is set to 0. As also mentioned in Section 4.2, ε is divided into ε_1 and ε_2 such that $\varepsilon_2 = w\varepsilon_1$ and $\varepsilon = \varepsilon_1 + \varepsilon_2$. The parameter w is computed by minimizing Equation 6 Lyu et al. [2017]. Table 4 lists w for different baselines, with its proof provided in Appendix G.

Table 4: Optimal Privacy Allocation. While ε is the overall privacy budget consumption, ε_1 and ε_2 are the privacy budget for threshold perturbation and query perturbation, respectively. w is an indicator of privacy budget allocation.

	SVT-Exp	SVT-Gum	SVT-Lap	SVT-Gau
ε	$\varepsilon = \varepsilon_1 + \varepsilon_2, \varepsilon_2 = w\varepsilon_1$			
w	$(\sqrt{2}c)^{2/3}$	$(\frac{\pi c}{\sqrt{3}})^{2/3}$	$(2c)^{2/3}$	$(2c)^{2/3}$

5.5 Evaluation Results

Hereinafter, we demonstrate the effectiveness of our proposed methods through experiments on six datasets, with an in-depth analysis of the evaluation results. Our main results, presented in Figure 7, show a significant advantage of Algorithm 2 over other baselines. The correctness and effectiveness of our optimal threshold correction method are shown in Table 5 and Figure 7. Finally, the effectiveness of our appending strategy and the trade-off it yields between efficiency and query accuracy is illustrated in Figure 8.

5.5.1 Effectiveness of Algorithm 2.

First, as illustrated in Figure 7, our proposed method (*i.e.*, SVT-Exp (optimal correction), shown with red-circle line) significantly outperforms others baselines by up to 50% on NCR across all tested privacy regions and datasets. Moreover, compared to other baselines, the performance of our proposed method closely matches the empirical SVT-Exp upper bound, further demonstrating its effectiveness. Second, our method shows a particular larger advantage when the gaps between predefined threshold and query results are relatively large (Cf. Figure 7(b) and Figure 6). This is because our threshold correction better filters out true positive queries far above the threshold, while our appending strategy effectively distinguishes smaller true positives from true negatives far below the threshold. Third, all compared variants, including ours, demonstrate higher NCR on datasets where the gaps between the threshold and query results are large even under smaller privacy budget (*e.g.*, $\varepsilon = 0.05$ on Kosarak), as these datasets are generally more robust to noise. Fourth, the NCR of other baselines decreases from SVT-Lap, SVT-Gumbel, to SVT-Gau, which aligns with our theoretical analysis in Figure 3 and Figure 4.

5.5.2 Effectiveness of the Optimal Threshold Correction

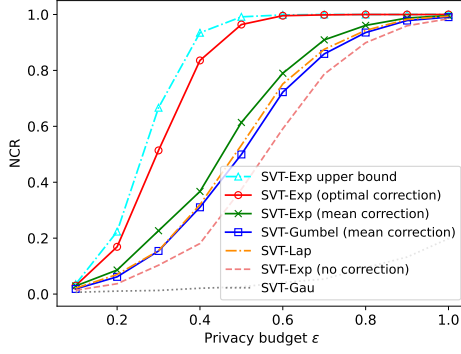
Table 5: Comparison of the threshold correction term between the optimal threshold correction method and the mean correction method, where $c = 50$ and $\alpha = 0$.

ε	0.01	0.05	0.1	1	2
Optimal	35450.45	7147.15	2803.30	280.78	138.89
Mean	5332.08	1046.42	523.21	52.32	26.16

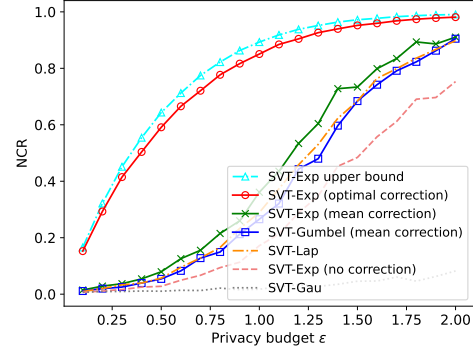
We compare our SVT-Exp (optimal correction) with SVT-Exp (mean correction) and SVT-Exp (no correction) in Figure 7, while Table 5 presents the values of optimal correction term r^{op} with different values of ε . First, as shown in Table 5, the optimal term is usually larger than the mean of the injected noise, aligning with our analysis in Section 4.3.2. Second, SVT-Exp without correction demonstrates relatively low NCR even compared to, *e.g.*, SVT-Lap, highlighting the need for a threshold correction method when using exponential noise in SVT. Third, SVT-Exp with our optimal correction terms drastically outperforms SVT-Exp with mean correction, which slightly outperforms the other baselines. This demonstrates the effectiveness of both exponential noise and optimal threshold correction methods.

5.5.3 Effectiveness of the Appending Strategy.

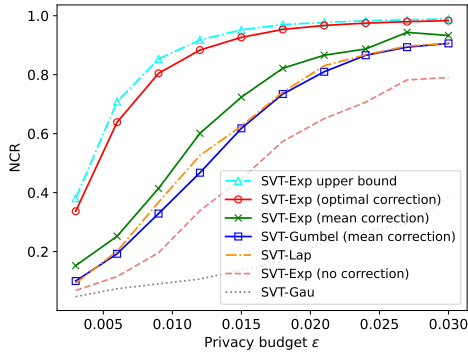
To demonstrate the effectiveness of our appending strategy, we compare the performance of all our baselines at the same overall privacy budget consumption with varying numbers of traverse (*i.e.*, the number of times a query with the noisy



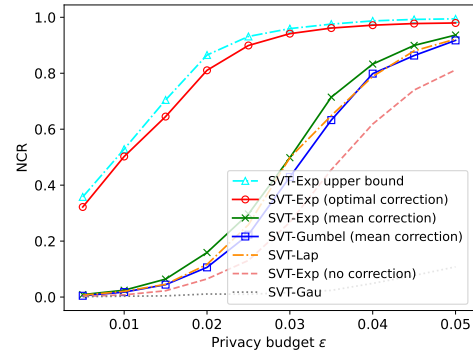
(a) Binary dataset



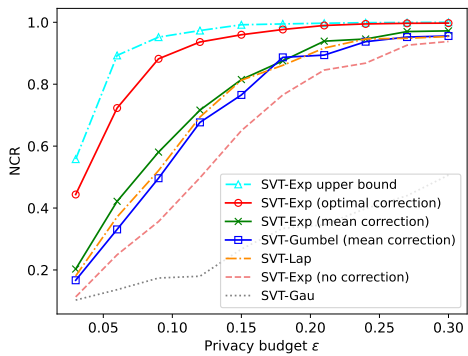
(b) Zipf dataset



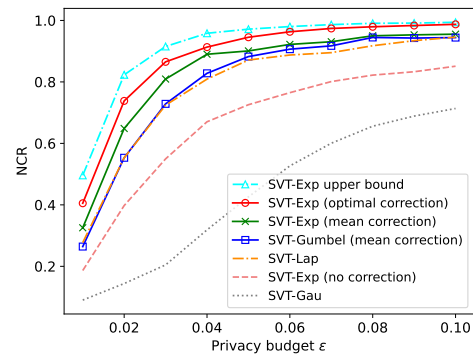
(c) BMS-POS dataset



(d) Kosarak dataset



(e) Adult dataset



(f) T40I10D100K dataset

Figure 7: NCR on six datasets with $c = 5$ for Adult dataset and $c = 50$ for the remaining datasets, $\alpha = 0$, $k = \lfloor \frac{m}{c} \rfloor$, $\text{RESAMPLE}=\text{False}$, and $\text{APPEND}=\text{True}$. Sequential composition theorem is adopted for computing ϵ .

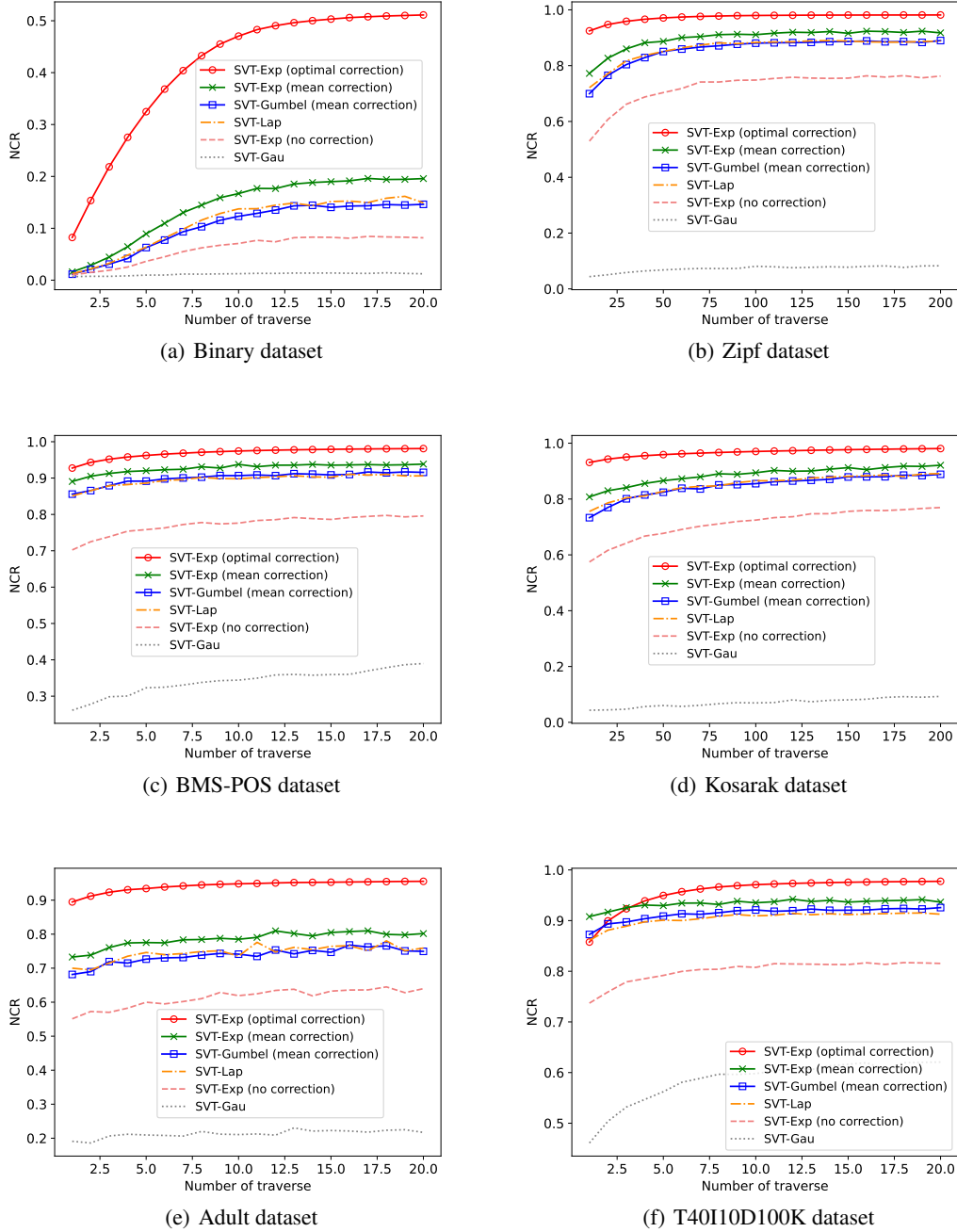


Figure 8: NCR on six datasets with varying number of traverses. Parameter c is set to 5 for Adult and 50 for the remaining datasets, $\alpha = 0$, $k = \lfloor \frac{m}{c} \rfloor$. RESAMPLE=False, and APPEND=True. Sequential composition theorem is adopted for computing ε .

negative outcome compared with the threshold)³. As shown in Figure 8, our proposed method performs better across most datasets under all tested traverse numbers. Notably, our method shows slight inferiority on the T40I10D100K dataset under a very small number of traverses. One possible reason is the relatively small gap between positive query results and the predefined threshold on T40I10D100K (Cf. Figure 6): due to our relatively high optimal threshold correction term, more queries are needed to filter out the true positive queries, as explained in Section 4.3.2. Even though, it is worth noting that our method outperforms the others on the T40I10D100K dataset with only a few more traverses (*e.g.*, less than 5). That is also to say, our proposed method yields better performance compared to other baselines with only a marginal additional computation cost.

6 Related Work

Our work focuses on enhancing one of the most fundamental DP algorithms initially introduced by Dwork et al. [2009, 2014], Roth and Roughgarden [2010], namely the sparse vector technique (SVT). Benefiting from its key feature where only positive outcomes consume privacy, SVT and its variants Kaplan et al. [2021] have become crucial components in numerous algorithms across various domains and scenarios Lee and Clifton [2014], Chen et al. [2015], Stoddard et al. [2014], Shokri and Shmatikov [2015], Bun et al. [2017], Hasidim et al. [2020], Zhang et al. [2021], Kaplan et al. [2023]. The applications of SVT span shared-parameter selection in deep learning models Shokri and Shmatikov [2015], time-stamp selection for streaming data Hasidim et al. [2020], online query answering Bun et al. [2017], among others. By improving the accuracy of SVT in a broad context, our work has the potential to enhance the performance of the aforementioned algorithms.

To gain deeper insights into the sparse vector technique, Lyu *et al.* summarize all prevalent SVT variants in Lyu et al. [2017]. Apart from the thorough privacy analysis under the classic notion of DP, they also propose an enhanced SVT with the optimal privacy budget allocation scheme. Shortly after, Zhu *et al.* Zhu and Wang [2020] revisit the privacy analysis of the SVT algorithm under a relaxed privacy notion, namely Rényi differential privacy (RDP) Mironov [2017]. Their research explores the utility of Gaussian noise for both threshold and query perturbation within the SVT framework. They argue that Gaussian noise may outperform Laplace noise in specific scenarios, such as when query results predominantly fall below predefined thresholds or when the number of queries is limited and not excessively large. In alignment with Lyu *et al.* Lyu et al. [2017], our work conducts the privacy analysis through the lens of DP, aiming for a generic result. Moreover, our work focuses more on noise selection rather privacy allocation, which distinguishes us from Lyu *et al.*. Also, we demonstrate the advantage of leveraging the exponential noise in comparison to other alternatives, which further distinguishes us from Zhu Zhu and Wang [2020].

Another line of research improves the SVT by exploiting information revealed in the algorithm for free. Concretely, Ding *et al.* Ding et al. [2023] pinpoint that releasing the gap between the noisy thresholds and the noisy query results incurs no extra privacy costs. Hence, they use the free gap as guidance to design a better privacy budget allocation scheme. Kaplan *et al.* Kaplan et al. [2021] improve SVT by iteratively deleting elements that contribute to current positive outcomes, which enables a more refined privacy accountant. Since both methods can be applied on top of our proposed method, we leave them out for comparison in this work.

Notice that we are not the pioneer effort in utilizing the exponential noise for achieving differential privacy in the literature. Previous studies from Durfee *et al.* Durfee and Rogers [2019] and Shekelyan *et al.* Shekelyan and Loukides [2022] demonstrate the use of exponential in achieving the exponential mechanism (EM), another differentially private algorithm primarily employed for privacy-preserving top-k selection tasks. Concretely, they Durfee and Rogers [2019], Shekelyan and Loukides [2022] leverage the exponential noise to Oneshot Qiao et al. [2021] mechanism where items with the top-k highest score are selected by injecting noise into each score ranking all noisy scores in descending order Wasserman and Zhou [2010], Ding et al. [2021], McKenna and Sheldon [2020]. While the exponential mechanism (EM) offers superior accuracy guarantees compared to SVT for the top-k selection problem, its application is limited: EM struggles with queries on streaming data, where the total number of queries might be infinite. Therefore, our focus remains on SVT in this work, given its broader applicability as a more generic algorithm. Ding *et al.* Ding et al. [2023] briefly look into applying the exponential noise to SVT. However, their approach, which involves injecting exponential noise into the threshold, has been demonstrated to compromise privacy by our findings. To the best of our knowledge, we are the first attempt that applies the exponential noise in SVT, accompanied by rigorous privacy and utility guarantee.

³For fairness, under each number of traverses, we ensure that each baseline consumes the same amount of the privacy budget before comparing their performance. Hence, the overall privacy budget consumption varies with a different number of traverses.

7 Conclusion

This work aims to enhance the query accuracy of the SVT algorithm by utilizing exponential noise. We begin with revisiting the privacy analysis of SVT algorithms and expanding the range of noise options for query perturbation by considering its less informative nature. Our analysis identifies exponential noise as the most effective, both theoretically and empirically, among the considered noise distributions. Additionally, we develop a generic optimal threshold correction method and an appending strategy to ensure both a high query precision and recall for SVT with marginal computation cost. The effectiveness of these methods is thoroughly validated through comprehensive experiments on both real-world and synthetic datasets.

A Proof of Theorem 2

Before starting our proof, we first define two different query settings for the SVT algorithm: the monotonic query setting and the non-monotonic query setting (or monotonic setting and non-monotonic setting in short).

For the monotonic setting, when the dataset D changes into its neighboring dataset D' , all the query results change in the same direction. That is to say, we have either $\forall_{i \in [n]} q_i(D) \geq q_i(D')$ or $\forall_{i \in [n]} q_i(D) \leq q_i(D')$, where n is number of different queries in total. By contrast, for the non-monotonic setting, the above statement is not necessary to be true: the query results can change in different directions when D changes into D' .

In the following, we first show our privacy analysis for the non-monotonic setting. We then elaborate on how to extend it to monotonic setting.

To begin with, we restate Theorem 2 as follows:

Theorem 5 (Restate of Theorem 2). *Algorithm 1 satisfies differential privacy if for any real numbers b_1, b_2 , there are two positive real numbers k_1 and k_2 such that the following inequalities hold:*

$$|\ln(f_1(x)) - \ln(f_1(x + b_1))| \leq k_1 |b_1|, \quad (10)$$

$$|\ln(1 - F_2(x)) - \ln(1 - F_2(x + b_2))| \leq k_2 |b_2|, \quad (11)$$

where $f_1(\cdot)$ and $F_2(\cdot)$ are the probability density function of \mathcal{N}_1 and the cumulative function of the \mathcal{N}_2 , respectively.

Now, we provide our proof under the non-monotonic settings.

Proof for the non-monotonic setting. Suppose there are a pair of neighboring datasets D and D' that differ by a single record, a sequence of n queries $Q = \{q_1, \dots, q_n\}$ that have the largest sensitivity Δ , and corresponding predefined thresholds $T = \{T_1, \dots, T_n\}$. Let \mathcal{M} denotes Algorithm 1, $o \in \mathcal{O}$ is a possible output, and S_\perp, S_\top denote the set of negative and positive outcomes, respectively. We have that

$$\begin{aligned} & \Pr[\mathcal{M}(D) = o] \\ &= \int_{-\infty}^{+\infty} \Pr[\rho = t] \Pr[\max_{i \in S_\perp} \tilde{q}_i(D) < \tilde{T}_i] \Pr[\min_{j \in S_\top} \tilde{q}_j(D) \geq \tilde{T}_j] dt \\ &= \int_{-\infty}^{+\infty} \Pr[\rho = t] \underbrace{\prod_{i \in S_\perp} \Pr[\tilde{q}_i(D) < \tilde{T}_i] \prod_{j \in S_\top} \Pr[\tilde{q}_j(D) \geq \tilde{T}_j]}_{(*)} dt, \end{aligned} \quad (12)$$

where $\tilde{q}_i(D) = q_i(D) + v_i$ and $\tilde{T}_i = T_i + \rho$ for each $i \in [n]$ are the perturbed query result and the perturbed threshold, respectively. In particular, t is an instance of the random variable ρ .

In the worst case, $0 \leq q_i(D') - q_i(D) \leq \Delta$ holds for $i \in S_\perp$ and $0 \leq q_j(D) - q_j(D') \leq \Delta$ holds for $j \in S_\top$. Therefore, it is further derived that

$$(*) \leq \prod_{i \in S_\perp} \Pr[\tilde{q}_i(D') - \Delta < \tilde{T}_i] \prod_{j \in S_\top} \Pr[\tilde{q}_j(D') + \Delta \geq \tilde{T}_j]. \quad (13)$$

By first inserting Inequality 13 into Equation 12 and then converting the integral variable t into $u = t + \Delta$, it is obvious that Equation 12 is no larger than

$$\int_{-\infty}^{+\infty} \Pr[\rho = t'] \underbrace{\prod_{i \in S_\perp} \Pr[\tilde{q}_i(D') < \tilde{T}_i] \prod_{j \in S_\top} \Pr[\tilde{q}_j(D') \geq \tilde{T}_j - 2\Delta]}_{(**)} du, \quad (14)$$

where $t' = u - \Delta$, $\tilde{T}_i = T_i + u$, and $\tilde{T}_j = T_j + u$.

If the distribution of the additive noise for threshold perturbation meets the condition in Theorem 2, by setting k_1 in Equation 10 to $\frac{\varepsilon_1}{|b_1|}$, we will therefore reach that

$$\Pr[\rho = t] \leq e^{\varepsilon_1} \cdot \Pr[\rho = t - \Delta]. \quad (15)$$

Additionally, notice that

$$(**) = \prod_{i \in S_{\perp}} F(\tilde{T}_i - q_i(D')) \prod_{j \in S_{\top}} (1 - F(\tilde{T}_j - 2\Delta - q_j(D'))), \quad (16)$$

where $F(\cdot)$ is the cumulative distribution function of the random noise v_i for $i \in [n]$ that is used for query results perturbation. If $F(\cdot)$ meets the condition stated by Inequality 11 in Theorem 2 and k is set to $\frac{\varepsilon_2}{|b||S_{\top}|}$, we obtain that for each $j \in S_{\top}$,

$$1 - F(\tilde{T}_j - 2\Delta - q_j(D')) \leq e^{\frac{\varepsilon_2}{c}} \cdot (1 - F(\tilde{T}_j - q_j(D'))), \quad (17)$$

where c is one of the inputs in Algorithm 1 and $|S_{\top}| \leq c$ holds. By converting the integral variable u back to t and putting all the pieces together, we finally have that

$$(12) \leq e^{\varepsilon_1 + \varepsilon_2} \cdot \int_{-\infty}^{+\infty} \Pr[\rho = t] \prod_{i \in S_{\perp}} F(\tilde{T}_i - q_i(D')) \prod_{j \in S_{\top}} (1 - F(\tilde{T}_j - q_j(D'))) dt = \Pr[\mathcal{M}(D') = o], \quad (18)$$

which then completes the proof. \square

Now, we show how we can extend our proof to the monotonic setting.

Proof for the monotonic setting. For the monotonic settings, the only difference lies in Inequality 13. As the worst case for this settings is that $0 \leq \tilde{q}_i(D') - \tilde{q}_i(D) \leq \Delta$ holds for $i \in S_{\perp}$, and $q_j(D) - q_j(D') = 0$ holds for $j \in S_{\top}$, we have that:

$$(*) \leq \prod_{i \in S_{\perp}} \Pr[\tilde{q}_i(D') - \Delta < \tilde{T}_i] \prod_{j \in S_{\top}} \Pr[\tilde{q}_j(D') \geq \tilde{T}_j]. \quad (19)$$

Then, similar to what we do under the non-monotonic setting, by first inserting Inequality 19 into Equation 12 and then converting the integral variable t into $u = t + \Delta$, we have that Equation 12 is no larger than

$$\int_{-\infty}^{+\infty} \Pr[\rho = t'] \underbrace{\prod_{i \in S_{\perp}} \Pr[\tilde{q}_i(D') < \tilde{T}_i] \prod_{j \in S_{\top}} \Pr[\tilde{q}_j(D') \geq \tilde{T}_j - \Delta]}_{(**)} du, \quad (20)$$

where $t' = u - \Delta$, $\tilde{T}_i = T_i + u$, and $\tilde{T}_j = T_j + u$. Then, we have that

$$(**) = \prod_{i \in S_{\perp}} F(\tilde{T}_i - q_i(D')) \prod_{j \in S_{\top}} (1 - F(\tilde{T}_j - \Delta - q_j(D'))), \quad (21)$$

holds. If $F(\cdot)$ meets the condition stated by Inequality 11 in Theorem 2, by setting k to $\frac{\varepsilon_2}{|b||S_{\top}|}$ and changing the integral variable u back to t , we are able to complete our proof as in Inequality 18. \square

B Proof of Theorem 3

Same as in Appendix A, we provide our proof of Theorem 3 first under the non-monotonic setting, then demonstrate how we can adapt Algorithm 2 as well as the privacy proof to the monotonic setting.

Theorem 6 (Restate of Theorem 3). *Let c denote the number of positive outcomes output by Algorithm 2. Algorithm 2 satisfies $(\varepsilon_1 + \varepsilon_2)$ -differential privacy when *RESAMPLE* is set to *False*, and $(c\varepsilon_1, \varepsilon_2)$ -differential privacy when *RESAMPLE* is set to *True*, where ε_1 and ε_2 are the privacy budgets for threshold and query perturbation, respectively.*

Proof. If RESAMPLE is set to FALSE, then based on the proof of Theorem 2, we only need to prove that cumulative distribution function (CDF) of the exponential distribution satisfies Equation 11. Since the CDF of the exponential distribution with parameter $\lambda = \frac{\varepsilon_2}{2c\Delta}$ is

$$F_{exp} = \begin{cases} 1 - \exp(-\lambda x) & x \geq 0, \\ 0 & \text{otherwise,} \end{cases} \quad (22)$$

we have that for each $j \in S_T$,

$$\begin{aligned} & \left| \ln(1 - F_{exp}(\tilde{T}_j - 2\Delta - q_j(D'))) - \ln(1 - F_{exp}(\tilde{T}_j - q_j(D'))) \right| \\ & \leq \left| \ln \frac{\exp(-\lambda(\tilde{T}_j - 2\Delta - q_j(D')))}{\exp(-\lambda(\tilde{T}_j - q_j(D')))} \right| \leq 2\Delta\lambda = \frac{\varepsilon_2}{c}, \end{aligned} \quad (23)$$

where c is the number of positive outcomes in Algorithm 2. In addition, as the Laplace noise is used for threshold perturbation, according to the Laplace mechanism described in Section 2.1, we have that

$$\Pr[\rho = t] \leq e_1^\varepsilon \cdot \Pr[\rho = t - \Delta]. \quad (24)$$

By plugging Equation 23 and Equation 24 into Equation 16 in Section 3, we arrive at the following inequalities:

$$\Pr[\mathcal{M}(D) = o] \leq e^{\varepsilon_1 + \varepsilon_2} \cdot \Pr[\mathcal{M}(D') = o], \quad (25)$$

which completes the proof when RESAMPLE = False.

If RESAMPLE is set to True, we can derive the privacy guarantee of Algorithm 2 by considering a subsequence of queries $\{q_1, \dots, q_k, q_{k+1}\}$ first. In particular, suppose the first k queries output negative outcomes while the $k + 1$ th query output a positive outcome. Then, we have that

$$\begin{aligned} & \Pr[\mathcal{M}_1(D) = o] \\ & = \int_{-\infty}^{+\infty} \Pr[\rho = t] \Pr[\max_{i=1}^k \tilde{q}_i(D) < \tilde{T}_i] \Pr[q_{k+1}(D) \geq \tilde{T}_{k+1}] dt \\ & = \int_{-\infty}^{+\infty} \Pr[\rho = t] \prod_{i=1}^k \Pr[\tilde{q}_i(D) < \tilde{T}_i] \Pr[q_{k+1}(D) \geq \tilde{T}_{k+1}] dt, \end{aligned} \quad (26)$$

where \mathcal{M}_1 is the the Algorithm 2 but with the sub-sequence mentioned above as inputs. Then, follow the same methodology as stated in Section 3, Equation 24, and Equation 23, it can be proved that

$$\Pr[\mathcal{M}_1(D) = o_1] \leq e^{\varepsilon_1 + \frac{\varepsilon_2}{c}} \cdot \Pr[\mathcal{M}_1(D)' = o_1]. \quad (27)$$

Notice that the original queries can be considered as a combination of c sub-sequences. By adopting the sequential composition theorem (*i.e.*, Theorem 1), we show that

$$\begin{aligned} & \Pr[\mathcal{M}(D) = o] = \Pr[(\mathcal{M}_1(D), \dots, \mathcal{M}_c(D)) = o] \\ & \leq e^{c(\varepsilon_1 + \frac{\varepsilon_2}{c})} \cdot \Pr[(\mathcal{M}_1(D)', \dots, \mathcal{M}_c(D)') = o] \\ & = e^{c\varepsilon_1 + \varepsilon_2} \cdot \Pr[\mathcal{M}(D') = o], \end{aligned} \quad (28)$$

which completes our proof. \square

Now, we elaborate on how we can adapt Algorithm 2 and its privacy proof to the monotonic setting.

As we have discussed in Appendix A, the only difference lies in Inequality 23. For the monotonic setting, for each $j \in S_T$, it holds that:

$$\begin{aligned} & \left| \ln(1 - F_{exp}(\tilde{T}_j - \Delta - q_j(D'))) - \ln(1 - F_{exp}(\tilde{T}_j - q_j(D'))) \right| \\ & \leq \left| \ln \frac{\exp(-\lambda(\tilde{T}_j - \Delta - q_j(D')))}{\exp(-\lambda(\tilde{T}_j - q_j(D')))} \right| \leq \Delta\lambda. \end{aligned} \quad (29)$$

Therefore, by perturbing each query result with random noise drawn from $\text{Exp}(\frac{1}{\lambda})$, where $\lambda = \frac{\varepsilon_2}{c\Delta}$, it is sufficient to provide a differential privacy guarantee stated in Theorem 3.

C Proof of Theorem 4

In this section, we first restate Theorem 4 in the following, then prove it in three steps. First, we formalize the (α, β) -accuracy in terms of Algorithm 2 in a simple case where only one positive query is allowed to output (*i.e.*, $c = 1$), $\Delta = 1$, and $\varepsilon_1 = \varepsilon_2 = \frac{\varepsilon}{2}$ as in Dwork et al. [2014]. Then, we provide the utility guarantee for the case where the threshold correction term r is set to 0. After that, we show that our optimal threshold correction term derived Equation 9 yields a accuracy no smaller than $r = 0$. Also note that our proof is under the non-monotonic query setting, and is trivial to extend it to the monotonic query setting.

Theorem 7 (Restate of Theorem 4). *Given any k records such that $|\{i < k : d_i \geq t - \alpha\}| = 0$ (*i.e.*, the record above and closest to the threshold is the last one), the Algorithm 2 at least $(\frac{4(\ln k + \ln \frac{2}{\beta})}{\varepsilon}, \beta)$ -accurate.*

Proof. As mentioned above, for ease of computation and comparison, without loss of generality, we assume that $\Delta = 1$, $c = 1$ and $\varepsilon_1 = \varepsilon_2 = \frac{\varepsilon}{2}$ in Algorithm 2.

Based on the definition of (α, β) -accuracy (Cf. Definition 3), we need to compute β given any α based on the following equation:

$$\begin{aligned} \beta &= 1 - \prod_{i=1}^k \Pr \left[\tilde{q}_i(D) - \alpha < \tilde{T}_i + r \right] \cdot \Pr \left[\tilde{q}_j(D) + \alpha \geq \tilde{T}_j + r \right] \\ &= 1 - p(r), \end{aligned} \quad (30)$$

where r is the threshold correction parameter and $p(r)$ is defined in Equation 7.

We first show that when $r = 0$, it holds that

$$\beta \leq 2 \exp \left(\frac{\ln k - \alpha \varepsilon}{4} \right) \quad (31)$$

Then, to prove Equation 31, it is sufficient for us to prove that with at least probability $1 - \beta$, the following inequality holds:

$$\max_{i \in [k]} \text{Exp}_i \left(\frac{4}{\varepsilon} \right) + \left| \text{Lap} \left(\frac{2}{\varepsilon} \right) \right| \leq \alpha, \quad (32)$$

where $\text{Exp}_i(\frac{1}{\lambda})$ is the random noise drawn from the exponential distribution with parameter λ and $\text{Lap}(b)$ is the random noise drawn from the Laplace distribution with parameter b .

If the above equation holds, for any i that $a_i = \top$, we have that

$$q_i(D) + \text{Exp}_i \left(\frac{4}{\varepsilon} \right) \geq \tilde{T}_i \geq T_i - \left| \text{Lap} \left(\frac{2}{\varepsilon} \right) \right|. \quad (33)$$

Or in other words:

$$q_i(D) \geq T_i - \left| \text{Lap} \left(\frac{2}{\varepsilon} \right) \right| - \text{Exp}_i \left(\frac{4}{\varepsilon} \right) \geq T_i - \alpha. \quad (34)$$

Similarly, for any $a_i = \perp$, we have that

$$q_i(D) \leq T_i + \left| \text{Lap} \left(\frac{2}{\varepsilon} \right) \right| + \text{Exp}_i \left(\frac{4}{\varepsilon} \right) \leq T_i + \alpha. \quad (35)$$

An error may occur when either $\text{Exp}_i(\frac{4}{\varepsilon})$ or $|\text{Lap}(\frac{2}{\varepsilon})|$ is too large. Since both errors could happen, $\frac{\alpha}{2}$ is allocate to each type Dwork et al. [2014]. Therefore, by letting the following inequalities hold:

$$\begin{aligned} \Pr \left[\min_{i \in [k]} \text{Exp}_i \left(\frac{4}{\varepsilon} \right) \geq \frac{\alpha}{2} \right] &\leq k \cdot \exp \left(-\frac{\alpha}{2} \right) \leq \frac{\beta}{2}, \\ \Pr \left[|\text{Lap}| \geq \frac{\alpha}{2} \right] &\leq \frac{\beta}{2}, \end{aligned} \quad (36)$$

together with some calculus, we have that Inequality 31 holds.

Now, we show that by taking the optimal threshold correction term r^{op} into consideration, there is a β' , such that

$$\beta' \leq \beta \leq 2 \exp \left(\frac{\ln k - \alpha \varepsilon}{4} \right) \quad (37)$$

holds.

Note that in Equation 9, the optimal threshold correction term r^{op} is obtained by maximizing $p(r)$. That is to say,

$$r^{op} = \arg \min (1 - \beta). \quad (38)$$

Hence, by inserting r^{op} back into Equation 30, we have that

$$\beta' = 1 - p(r^{op}) \leq 1 - p(r) = \beta \quad (39)$$

holds. Our proof of Theorem 4 is then completed by computing α based on Inequality 37. \square

D Analytical Expression of $p(r)$

By inserting $r + \alpha$ and $r - \alpha$ into Equation 10 in Cahillane [2024], we obtain the following equations immediately:

$$p(r) = (\Gamma(r + \alpha))^k \cdot (1 - \Gamma(r - \alpha))$$

$$= \begin{cases} \left(\frac{b \exp\left(\frac{r+\alpha}{b}\right)}{2(1/\lambda+b)} \right)^k \left(1 - \frac{b \exp\left(\frac{r-\alpha}{b}\right)}{2(1/\lambda+b)} \right) & r \leq -\alpha, \\ \left(1 + \frac{(1/\lambda)^2 \exp\left(-\frac{r+\alpha}{1/\lambda}\right) - b \exp\left(-\frac{r+\alpha}{b}\right)}{b^2 - (1/\lambda)^2} - \frac{b \exp\left(-\frac{r+\alpha}{b}\right)}{2(b-1/\lambda)} \right)^k \left(1 - \frac{b \exp\left(\frac{r-\alpha}{b}\right)}{2(1/\lambda+b)} \right) & -\alpha \leq r \leq \alpha, \\ \left(1 + \frac{(1/\lambda)^2 \exp\left(-\frac{r+\alpha}{1/\lambda}\right) - b \exp\left(-\frac{r+\alpha}{b}\right)}{b^2 - (1/\lambda)^2} - \frac{b \exp\left(-\frac{r+\alpha}{b}\right)}{2(b-1/\lambda)} \right)^k \left(-\frac{(1/\lambda)^2 \exp\left(-\frac{r-\alpha}{1/\lambda}\right) + b \exp\left(-\frac{r-\alpha}{b}\right)}{b^2 - (1/\lambda)^2} + \frac{b \exp\left(-\frac{r-\alpha}{b}\right)}{2(b-1/\lambda)} \right) & r > \alpha, \end{cases} \quad (40)$$

where $b = \frac{\Delta}{\varepsilon_1}$ and $\lambda = \frac{\varepsilon_2}{2c\Delta}$ for the non-monotonic query setting, $b = \frac{\Delta}{\varepsilon_1}$ and $\lambda = \frac{\varepsilon_2}{c\Delta}$ for the monotonic query setting respectively.

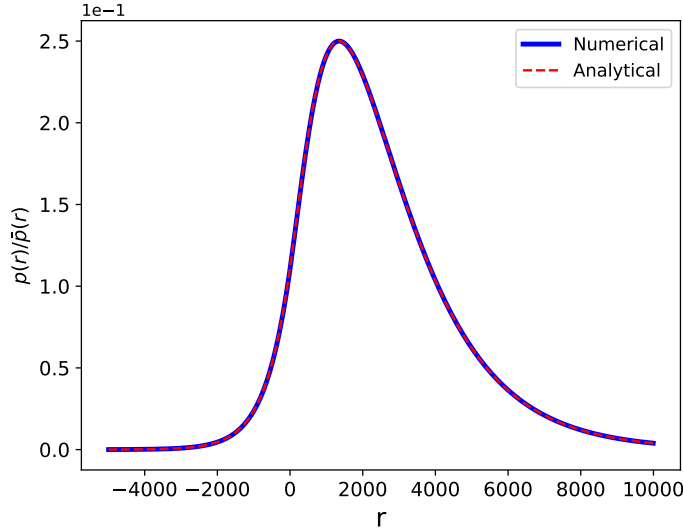


Figure 9: Comparison of $\bar{p}(r)$ computed using Algorithm 3 and Algorithm 4. The bucket size m Algorithm 4 is set to 20,001. The other involved parameters are set as $\varepsilon = 0.03$, $\alpha = 0$, $k = 10$.

We compare the analytical expression of $p(r)$ presented in Equation 40 with our numerical estimation computed using Algorithm 3 and Algorithm 4 in Figure 9 to demonstrate the correctness of our numerical framework. The comparison shows that the numerical result align with the analytical expression, validating the correctness of both numerical framework and analytical result.

E Proof of the Maximum Value of $p(r)$

To justify the design of our optimal threshold correction method, we prove in Theorem 8 that for any pair of noise distributions, the maximum value of $p(r)$ exists. Consequently, we can always obtain the optimal threshold correction term r^{op} by maximizing $p(r)$.

Theorem 8. *The maximum value of $p(r)$ exists and is no smaller than $\frac{k^k}{(k+1)^{k+1}}$.*

Proof. According to Equation 8, we have:

$$p(r) = (\Gamma(r + \alpha))^k \cdot (1 - \Gamma(r - \alpha)), \quad (41)$$

the differentiation of which is written as:

$$p'(r) = (\Gamma(r + \alpha))^{k-1} \cdot (kf(r + \alpha)(1 - \Gamma(r - \alpha)) - \Gamma(r + \alpha)f(r - \alpha)), \quad (42)$$

where $f(\cdot)$ is the probability density function of the $\Gamma(\cdot)$. As $\Gamma(r + \alpha)^{k-1} > 0$ holds, when $r \rightarrow -\infty$, both $\Gamma(r - \alpha)$ and $\Gamma(r + \alpha)$ grow closer to 0. In other words:

$$\lim_{r \rightarrow -\infty} p'(r) = f(r + \alpha) \geq 0. \quad (43)$$

Similarly, when $r \rightarrow +\infty$, we have $\Gamma(r + \alpha) \rightarrow 1$ and $\Gamma(r - \alpha) \rightarrow 1$. Therefore, we have:

$$\lim_{r \rightarrow +\infty} p'(r) = -f(r - \alpha) \leq 0. \quad (44)$$

Since $p'(r)$ is a continuous function for $r \in \mathbb{R}$, there must be a r that has $p'(r) = 0$. Also, we have the following inequalities hold for any $r \in \mathbb{R}$ and $\alpha \geq 0$:

$$\begin{aligned} p(r) &= (\Gamma(r + \alpha))^k \cdot (1 - \Gamma(r - \alpha)) \\ &\geq \underbrace{\Gamma(r)^k \cdot (1 - \Gamma(r))}_{(***)}. \end{aligned} \quad (45)$$

Since the maximum value of $(***)$ is $\frac{k^k}{(k+1)^{k+1}}$, which can be achieved when $\Gamma(r) = \frac{k}{k+1}$, we have that the maximum value of $p(r)$ is no less than $\frac{k^k}{(k+1)^{k+1}}$ according to Equation 45, which completes our proof. \square

F Privacy Analysis of SVT-Gum

To start with, we present the pseudo-code of the SVT algorithm with Gumbel noise in the Algorithm 5.

Algorithm 5: SVT with Gumbel noise.

Input: $Q = \{q_1, q_2, \dots\}, \Delta, \varepsilon_1, \varepsilon_2, \lambda, c, T = \{T_1, T_2, \dots\}, \gamma, \varepsilon, m$, option RESAMPLE

```

1  $\rho \sim Lap(0, \frac{\Delta}{\varepsilon_1});$ 
2  $n_c = 0; n_a = 0;$ 
3  $r = \text{CorrectionTermOptimization}(b, \lambda, \gamma);$ 
4 for  $i = 1, 2, 3, \dots$  do
5    $n_a = n_a + 1;$ 
6    $\beta = \frac{2c\Delta}{\varepsilon_2}; v_i \sim Gum(0, \beta);$ 
7   if  $q_i(D) + v_i \geq \rho + T_i + r$  then
8     Output  $a_i = \top;$ 
9      $n_c = n_c + 1;$ 
10     $S_\top = S_\top \cup i;$ 
11    if RESAMPLE,  $\rho \sim Lap(0, \frac{\Delta}{\varepsilon_1});$ 
12    Abort if  $n_c \geq c;$ 
13  else
14    Output  $a_i = \perp$ 
15  end
16 end

```

Notice that the only difference between the Algorithm 2 and the Algorithm 5 is that we use the random noise drawn from the Gumbel distribution with parameter $\beta = \frac{2c\Delta}{\varepsilon_2}$. In particular, the cumulative function of this distribution is:

$$F_{Gum}(x) = \exp(-\exp(-\frac{x}{\beta})). \quad (46)$$

The privacy of Algorithm is given in the following theorem:

Theorem 9 (Privacy guarantee). *Algorithm 5 satisfies $(\varepsilon_1 + \varepsilon_2)$ -differential privacy when RESAMPLE is set to False, and $(c\varepsilon_1, \varepsilon_2)$ -differential privacy when RESAMPLE is set to True.*

Proof. To prove Theorem 9, we only need to show that $F_{Gum}(x)$ satisfies the condition in Theorem 2. In other words, we have to prove that

$$\left| \frac{1 - \exp(-\exp(-\frac{x}{\beta}))}{1 - \exp(-\exp(-\frac{x+2\Delta}{\beta}))} \right| \leq e^{\frac{\varepsilon_2}{c}}. \quad (47)$$

For simplicity, we remove the symbol of absolute value here as the $\left| \frac{1-F(x+c)}{1-F(x)} \right| \geq e^{-\frac{\varepsilon_2}{c}}$ follows by symmetry.

For clarity, we let a denote $-\exp(-\frac{x}{\beta})$ and b denote $\exp(-\varepsilon)$. Therefore, to prove that Equation 47 holds for any $\varepsilon_2 \geq 0$, we only need to show that the following equation holds:

$$1 - \exp(ab) - b(1 - \exp(a)) \geq 0. \quad (48)$$

In particular, we let:

$$f(b) = 1 - \exp(ab) - b(1 - \exp(a)). \quad (49)$$

Then, we have

$$f'(b) = 1 - a \exp(ab) - (1 - \exp(a)) \geq 0 \quad (50)$$

holds for any $x \in \mathbb{R}$ and any $\varepsilon_2 \geq 0$. Therefore, we have that when $b = 0$, $f(b)$ takes the minimum value, which is 0. The Equation 47 is then proved. The rest of the proof of Theorem 9 follows the same methodology as the proof of Theorem 3. We hence omit it from here for simplicity. Also note that our proof here is for the non-monotonic query setting. The privacy analysis for the monotonic query setting can be developed follow the same methodology as in Appendix B, we also omit it from here. \square

G Proof of Privacy Allocation

Overall, the optimal privacy budget allocation scheme follows the methodology proposed by Lyu *et al.* Lyu et al. [2017]: to make the following comparison as accurate as possible, we need to minimize the variance $V = \text{Var}(N_1) + \text{Var}(N_2)$.

$$q(D) + N_2(c, \varepsilon_2) \geq T + N_1(c, \varepsilon_1). \quad (51)$$

In this section, we discuss the optimal privacy budget allocation results with different noise distributions for the non-monotonic query setting. We omit the proof for the monotonic query setting, as it shares the same methodology and similar calculations as its non-monotonic counterparts. However, we provide the optimal privacy allocation results for monotonic query settings in Table 6 to offer additional insights.

Table 6: Optimal Privacy Allocation for the Monotonic Query Setting. While ε is the overall privacy budget consumption, ε_1 and ε_2 are the privacy budget for threshold perturbation and query perturbation, respectively. w is an indicator for privacy budget allocation.

	SVT-Exp	SVT-Gum	SVT-Lap	SVT-Gau
ε	$\varepsilon = \varepsilon_1 + \varepsilon_2, \varepsilon_2 = w\varepsilon_1$			
w	$\left(\frac{c}{\sqrt{2}}\right)^{2/3}$	$\left(\frac{\pi c}{2\sqrt{3}}\right)^{2/3}$	$c^{2/3}$	$c^{2/3}$

G.1 SVT-Exp

In SVT-Exp, $N_1(c, \varepsilon_1) = \text{Lap}(\frac{\Delta}{\varepsilon_1})$ and $N_2(c, \varepsilon_2) = \text{Exp}(\frac{2c\Delta}{\varepsilon_2})$. Thus, we have that

$$V = 2 \left(\frac{\Delta}{\varepsilon_1} \right)^2 + \left(\frac{2c\Delta}{\varepsilon_2} \right)^2. \quad (52)$$

Let $\varepsilon = \varepsilon_1 + \varepsilon_2$ and $\varepsilon_2 = k\varepsilon_1$, V can be written as

$$V = 2 \left(\frac{(w+1)\Delta}{\varepsilon} \right)^2 + \left(\frac{2c(w+1)\Delta}{w\varepsilon} \right)^2. \quad (53)$$

After some calculation, it is derived that V is minimized when w is set to $(\sqrt{2}c)^{2/3}$.

G.2 SVT-Gum

In SVT-Gum, $N_1(c, \varepsilon_1) = \text{Lap}(\frac{\Delta}{\varepsilon_1})$ and $N_2(c, \varepsilon_2) = \text{Gum}(\frac{2c\Delta}{\varepsilon_2})$. Thus, we have that

$$V = 2 \left(\frac{\Delta}{\varepsilon_1} \right)^2 + \frac{\pi^2}{6} \left(\frac{2c\Delta}{\varepsilon_2} \right)^2. \quad (54)$$

Let $\varepsilon = \varepsilon_1 + \varepsilon_2$ and $\varepsilon_2 = w\varepsilon_1$, V can be written as

$$V = 2 \left(\frac{(w+1)\Delta}{\varepsilon} \right)^2 + \frac{\pi^2}{6} \left(\frac{2c(w+1)\Delta}{w\varepsilon} \right)^2. \quad (55)$$

After some calculation, it is derived that V is minimized when w is set to $(\frac{\pi c}{\sqrt{3}})^{2/3}$.

G.3 SVT-Lap

In SVT-Lap, $N_1(c, \varepsilon_1) = \text{Lap}(\frac{\Delta}{\varepsilon_1})$ and $N_2(c, \varepsilon_2) = \text{Lap}(\frac{2c\Delta}{\varepsilon_2})$. Thus, we have that

$$V = 2 \left(\frac{\Delta}{\varepsilon_1} \right)^2 + 2 \left(\frac{2c\Delta}{\varepsilon_2} \right)^2. \quad (56)$$

Let $\varepsilon = \varepsilon_1 + \varepsilon_2$ and $\varepsilon_2 = w\varepsilon_1$, V can be written as

$$V = 2 \left(\frac{(w+1)\Delta}{\varepsilon} \right)^2 + 2 \left(\frac{2c(w+1)\Delta}{w\varepsilon} \right)^2. \quad (57)$$

After some calculation, it is derived that V is minimized when w is set to $(2c)^{2/3}$.

G.4 SVT-Gau

In SVT-Gau, we assume that $\sigma = \frac{\alpha\Delta}{\varepsilon}$ Dwork et al. [2014]. Therefore, we have that the variance of $N_1(c, \varepsilon_1)$ is $\sigma_1^2 = \left(\frac{\alpha\Delta}{\varepsilon_1} \right)^2$ and the variance of $N_2(c, \varepsilon_2)$ is $\sigma_2^2 = \left(\frac{2\alpha c\Delta}{\varepsilon_2} \right)^2$. In other words, we have that

$$V = \sigma_1^2 + \sigma_2^2 = \left(\frac{\alpha\Delta}{\varepsilon_1} \right)^2 + \left(\frac{2\alpha c\Delta}{\varepsilon_2} \right)^2. \quad (58)$$

Let $\varepsilon = \varepsilon_1 + \varepsilon_2$ and $\varepsilon_2 = w\varepsilon_1$, V can be written as

$$V = \left(\frac{(w+1)\alpha\Delta}{\varepsilon} \right)^2 + \left(\frac{2\alpha c(w+1)\Delta}{w\varepsilon} \right)^2. \quad (59)$$

After some calculation, it is derived that V is minimized when w is set to $(2c)^{2/3}$.

H Evaluation Results over F1-score

In this section, we first present the overall evaluation results for the F1-score across six datasets in Figure 10, which exhibits similar trends to those observed for NCR in Figure 7. We then analyze how the F1-score varies with the increasing number of traverses for queries with negative noisy outcomes in Figure 11. This analysis also reflects similar trends and provides comparable insights to those observed in Figure 8.

I Evaluation Results under RDP Composition

In this section, we provide the empirical evaluation results under RDP composition as mentioned in Section 2.1. We first specify the experiment settings, and then present the evaluation results in Figure 12, Figure 13, Figure 14, and Figure 15, respectively.

Parameter settings. As stated by Zhu *et al.* Zhu and Wang [2020], using RDP composition in SVT results in a failure rate in Definition 1 that is greater than 0. In this section, we set the failure rate δ to $\frac{1}{n}$ for all compared baselines, following convention Dwork et al. [2014]. For the overall privacy budget allocation, we adhere to the rules in

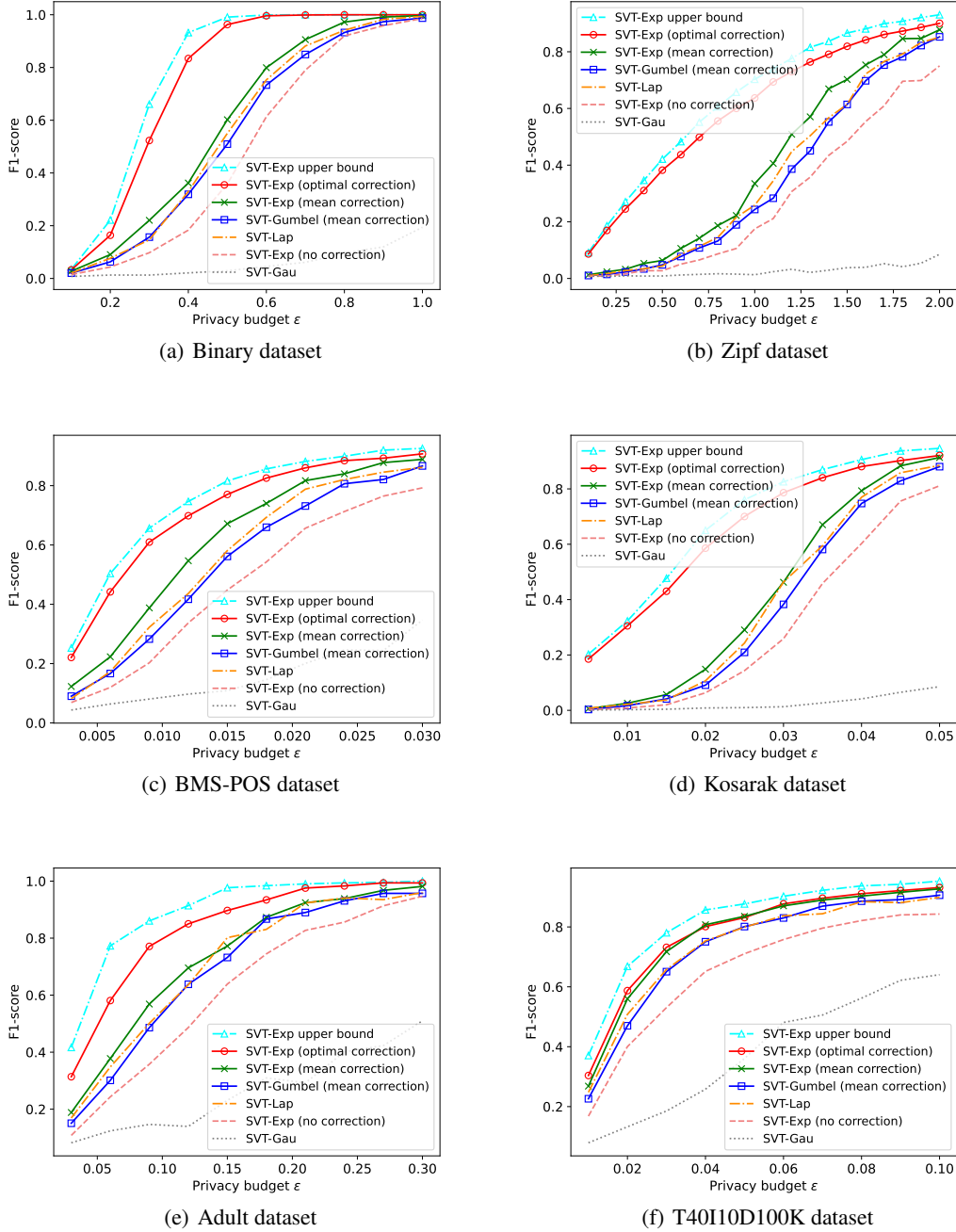


Figure 10: F1-score on six datasets with $c = 5$ for Adult and $c = 50$ for the remaining datasets, $\alpha = 0$, $k = \lfloor \frac{m}{c} \rfloor$, RESAMPLE=False, and APPEND=True. The sequential composition theorem is adopted for the overall privacy budget (*i.e.*, ϵ) computation.

Section 5.4. Specifically, for a fixed overall privacy budget ε , we use binary search to determine ε_1 and ε_2 such that $\varepsilon_1 + \varepsilon_2 = \varepsilon$, $\varepsilon_2 = w\varepsilon_1$, and accumulated privacy budget for c noisy positive outcomes equals to ε_2 after applying the RDP composition theorem when each query is assigned a privacy budget ε'_2 . Additionally, we provide the evaluation results on only three datasets: Binary, BMS-POS, and Kosarak, as similar trends exhibit on other datasets. This selective presentation ensures clarity while maintaining the comprehensiveness of our analysis.

Evaluation results. The results for NCR and F1-score of Algorithm 2 under RDP composition are presented in Figure 12 and Figure 13, respectively. First, our proposed method consistently outperforms the other baselines across all datasets and privacy regions, similar to the trends observed in Figure 7 and Figure 10, where the sequential composition theorem is adopted. This further demonstrates the effectiveness of our proposed method as well as the generality of our method to other relevant techniques in the literature. Second, the performance for both the F1-score and NCR of all compared baselines improves compared to their sequential composition counterparts. Notably, SVT-Gau shows a larger performance increase relative to the other baselines. This finding aligns with the analysis provided by Zhu *et al.* Zhu and Wang [2020], which highlights that Gaussian noise achieves tighter composition results with RDP composition compared to other noise types. However, contrary to their results where SVT-Gau outperforms SVT-Lap, our results show that SVT-Lap still maintains a significant advantage. This discrepancy can be attributed to the different tested scenarios. As discussed by Zhu *et al.*, SVT-Gau is more suitable for scenarios where the gap between query results and predefined thresholds is relatively large, and relatively few queries are made. In our settings, however, many query results are quite close to the predefined threshold, and a large number of queries are conducted. This context reduces the relative effectiveness of SVT-Gau compared to SVT-Lap.

Figure 14 and Figure 15 illustrate the trade-off between query accuracy and efficiency for our method under RDP composition. Consistent with the results shown in Figure 8 and Figure 11, our proposed method outperforms the other baselines across most datasets for all tested numbers of traversals. For the remaining datasets, our method demonstrates significant improvements in query accuracy and surpasses other baselines after a few additional rounds of traversals. This highlights the effectiveness of our appending strategy and confirms that our proposed method achieves superior query accuracy with only a marginal additional computational cost.

J Impact of the Error Tolerance Parameter

In this section, we analyze how the error tolerance parameter α in Equation 8 affects the query accuracy of our proposed method. Specifically, we present the NCR of our method with varying values of α on the Binary dataset, using the sequential composition theorem, as shown in Figure 16. Figure 16 demonstrates that our method remains robust to different values of α due to the effectiveness of the appending strategy. This robustness implies that setting α to 0 across various data distributions generally yields satisfactory performance. However, it is important to note that a higher success probability in Figure 5(c) does not always correspond to a higher NCR. As discussed in Section 4.3.2, a larger α increases the success probability by allowing more queries to be mistakenly classified, which can lead to a decrease in NCR. For the Binary dataset, setting α to 500, which is equal to the gap between query results and the predefined threshold, results in slightly better performance compared to other settings. The rationale behind this is straightforward: increasing α within the range $[0, |q(D) - T|]$ does not negatively impact accuracy, as no query result falls within this interval. Thus, this choice of α optimizes the trade-off between accuracy and error tolerance in this particular context.

K Computation Efficiency of the Optimal Threshold Correction Term

In this section, we analyze the trade-off between the running time of our numerical optimal threshold correction framework and the accuracy of the estimated optimal threshold correction term r^{op} , which is derived from the success probability $p(r)$ in Equation 8. The primary computational cost of our numerical framework arises from the convolution between two discretized distributions. The time complexity for this convolution is $o(m \log(m))$, where m represents the bucket size in Algorithm 3 and Algorithm 4. Figure 17 illustrates the running time of our numerical framework as the bucket size increases, compared to the running time of the analytical computation using Equation 40. The figure shows that while the analytical computation time remains constant regardless of bucket size, the running time of our numerical framework increases linearly with the bucket size. Meanwhile, the l_2 norm of the estimation error of $\bar{p}(r)$ in Algorithm 3 decreases drastically as the bucket size increases. However, it is also worth noting that even with the smallest bucket size tested in Figure 17 that incurs only less than 0.01 seconds of additional computation cost, our numerical framework achieves a l_2 norm error in the estimation of $\bar{p}(r)$ of less than 0.01. This estimation error scale on $\bar{p}(r)$ leads to almost no estimation error on \bar{r}^{op} . This is also to say, that our numerical framework achieves a very high estimation accuracy on \bar{r}^{op} with only a marginal additional computation cost.

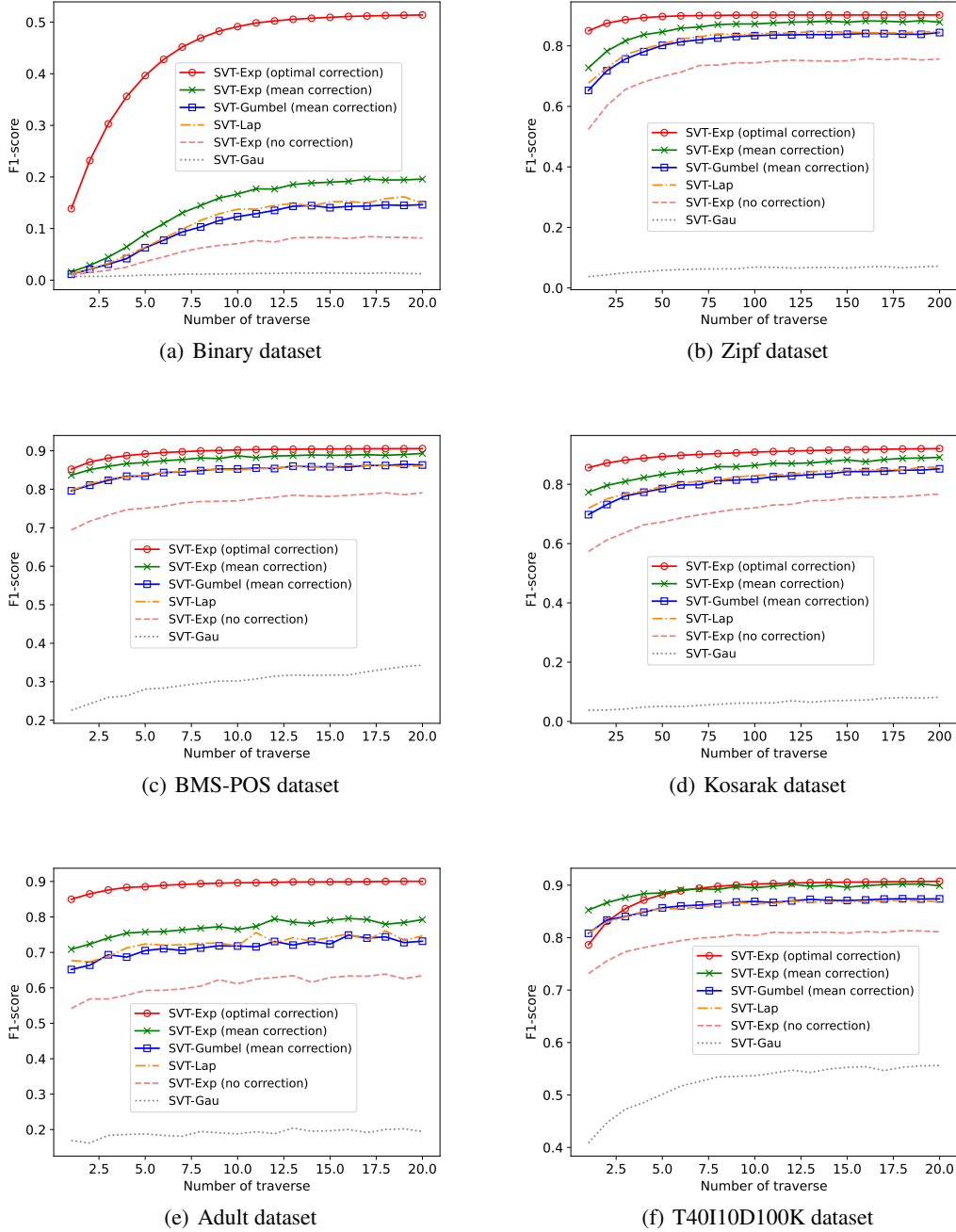


Figure 11: F1-score on six datasets under varying number of traverses with $c = 5$ for Adult and $c = 50$ for the remaining datasets, $\alpha = 0$, $k = \lfloor \frac{m}{c} \rfloor$. RESAMPLE=False, and APPEND=True. The sequential composition theorem is adopted for the overall privacy budget (*i.e.*, ϵ) computation.

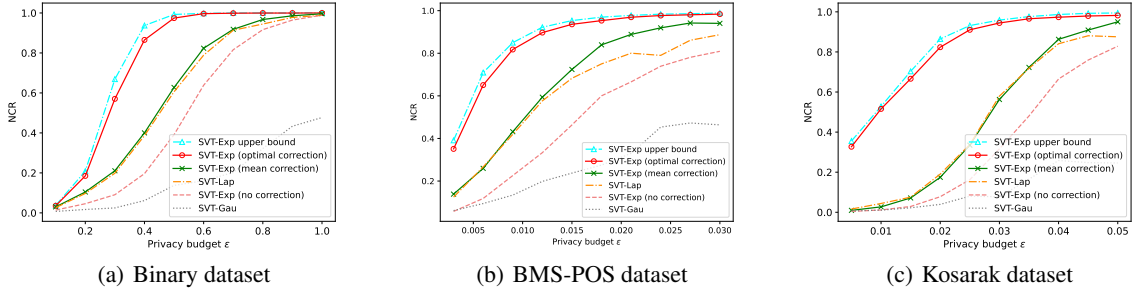


Figure 12: NCR on three datasets with $c = 50$, $\alpha = 0$, $k = \lfloor \frac{m}{c} \rfloor$, RESAMPLE=False, and APPEND=True. The RDP composition theorem is adopted for the overall privacy budget (i.e., ϵ) computation.

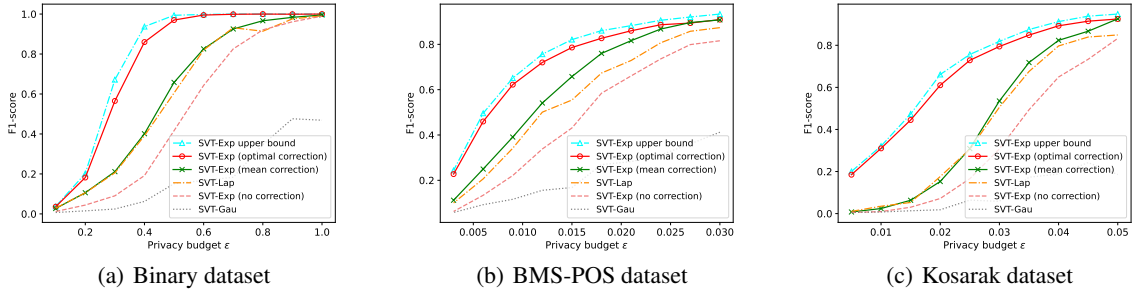


Figure 13: F1-score on three datasets with $c = 50$, $\alpha = 0$, $k = \lfloor \frac{m}{c} \rfloor$, RESAMPLE=False, and APPEND=True. The RDP composition theorem is adopted for the overall privacy budget (i.e., ϵ) computation.

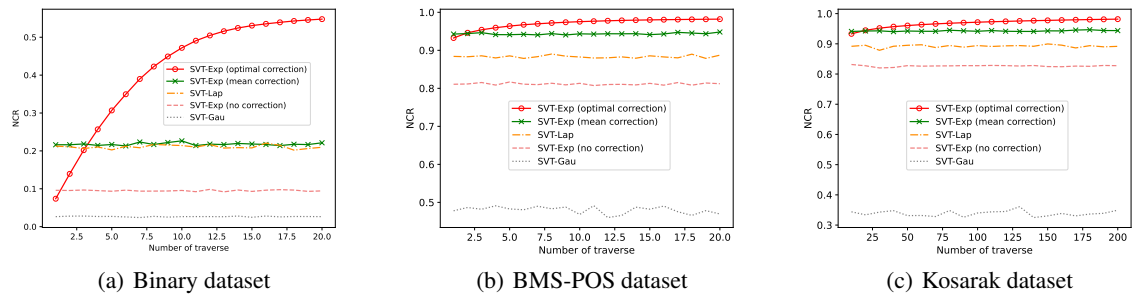


Figure 14: NCR on three datasets under varying number of traverse with $c = 50$, $\alpha = 0$, $k = \lfloor \frac{m}{c} \rfloor$. The RDP composition theorem is adopted for the overall privacy budget (i.e., ϵ) computation.

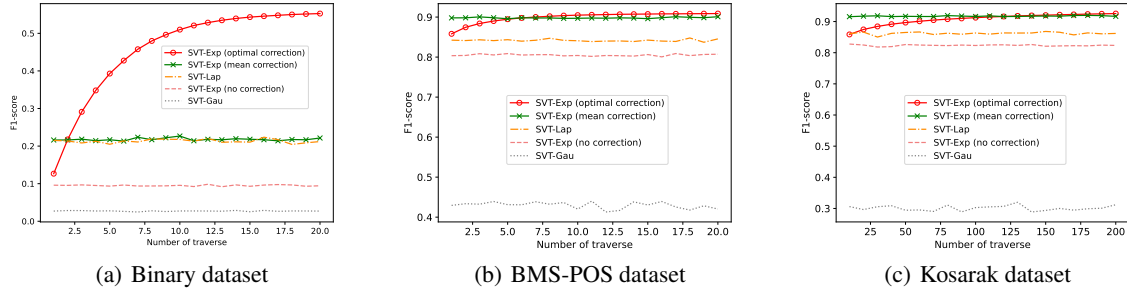


Figure 15: F1-score on three datasets under varying number of traverse with $c = 50$, $\alpha = 0$, $k = \lfloor \frac{m}{c} \rfloor$. The RDP composition theorem is adopted for the overall privacy budget (*i.e.*, ϵ) computation.

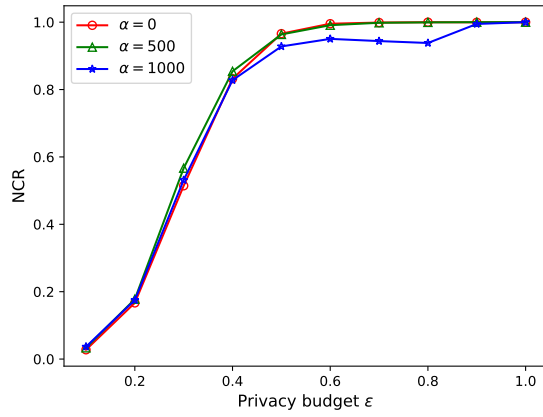


Figure 16: NCR of Algorithm 2 with varying α on Binary dataset. The parameter c is set to 50, and the overall privacy budget ϵ ranges from 0.1 to 1.0.

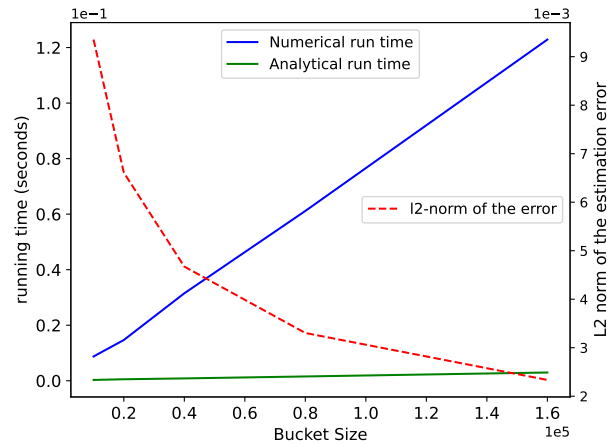


Figure 17: The trade-off of the numerical threshold correction method between estimation accuracy of $\hat{p}(r)$ in Algorithm 3 and the algorithm running time.

References

- Cynthia Dwork, Moni Naor, Omer Reingold, Guy N Rothblum, and Salil Vadhan. On the complexity of differentially private data release: efficient algorithms and hardness results. In *Proceedings of the forty-first annual ACM symposium on Theory of computing*, pages 381–390, 2009.
- Cynthia Dwork, Aaron Roth, et al. The algorithmic foundations of differential privacy. *Foundations and Trends® in Theoretical Computer Science*, 9(3–4):211–407, 2014.
- Raef Bassily, Om Thakkar, and Abhradeep Guha Thakurta. Model-agnostic private learning. *Advances in Neural Information Processing Systems*, 31, 2018.
- Avinatan Hasidim, Haim Kaplan, Yishay Mansour, Yossi Matias, and Uri Stemmer. Adversarially robust streaming algorithms via differential privacy. *Advances in Neural Information Processing Systems*, 33:147–158, 2020.
- Min Lyu, Dong Su, and Ninghui Li. Understanding the sparse vector technique for differential privacy. *Proceedings of the VLDB Endowment*, 10(6), 2017.
- Yuqing Zhu and Yu-Xiang Wang. Improving sparse vector technique with renyi differential privacy. *Advances in Neural Information Processing Systems*, 33:20249–20258, 2020.
- Úlfar Erlingsson, Vasyl Pihur, and Aleksandra Korolova. Rappor: Randomized aggregatable privacy-preserving ordinal response. In *Proceedings of the 2014 ACM SIGSAC conference on computer and communications security*, pages 1054–1067, 2014.
- Cynthia Dwork. Differential privacy. In *International colloquium on automata, languages, and programming*, pages 1–12. Springer, 2006.
- Quan Geng, Wei Ding, Ruiqi Guo, and Sanjiv Kumar. Optimal noise-adding mechanism in additive differential privacy. In *The 22nd International Conference on Artificial Intelligence and Statistics*, pages 11–20. PMLR, 2019.
- Cynthia Dwork, Guy N Rothblum, and Salil Vadhan. Boosting and differential privacy. In *2010 IEEE 51st annual symposium on foundations of computer science*, pages 51–60. IEEE, 2010.
- Peter Kairouz, Sewoong Oh, and Pramod Viswanath. The composition theorem for differential privacy. In *International conference on machine learning*, pages 1376–1385. PMLR, 2015.
- Sebastian Meiser and Esfandiar Mohammadi. Tight on budget? tight bounds for r-fold approximate differential privacy. In *Proceedings of the 2018 ACM SIGSAC Conference on Computer and Communications Security*, pages 247–264, 2018.
- Sivakanth Gopi, Yin Tat Lee, and Lukas Wutschitz. Numerical composition of differential privacy. *Advances in Neural Information Processing Systems*, 34:11631–11642, 2021.
- Ilya Mironov. Rényi differential privacy. In *2017 IEEE 30th computer security foundations symposium (CSF)*, pages 263–275. IEEE, 2017.
- Tianhao Wang, Jeremiah Blocki, Ninghui Li, and Somesh Jha. Locally differentially private protocols for frequency estimation. In *26th USENIX Security Symposium (USENIX Security 17)*, pages 729–745, 2017.
- Qingqing Ye, Haibo Hu, Xiaofeng Meng, and Huadi Zheng. Privkv: Key-value data collection with local differential privacy. In *2019 IEEE Symposium on Security and Privacy (SP)*, pages 317–331. IEEE, 2019.
- Yuhan Liu, Suyun Zhao, Yixuan Liu, Dan Zhao, Hong Chen, and Cuiping Li. Collecting triangle counts with edge relationship local differential privacy. In *2022 IEEE 38th International Conference on Data Engineering (ICDE)*, pages 2008–2020. IEEE, 2022.
- Yixuan Liu, Suyun Zhao, Li Xiong, Yuhan Liu, and Hong Chen. Echo of neighbors: Privacy amplification for personalized private federated learning with shuffle model. *arXiv preprint arXiv:2304.05516*, 2023.
- Henri J Nussbaumer and Henri J Nussbaumer. *The fast Fourier transform*. Springer, 1982.
- Omid Shakeri and Mir Pedram. QtyT40I10D100K. UCI Machine Learning Repository, 2012. DOI: <https://doi.org/10.24432/C5360W>.
- Zijian Zheng, Ron Kohavi, and Llew Mason. Real world performance of association rule algorithms. In *Proceedings of the seventh ACM SIGKDD international conference on Knowledge discovery and data mining*, pages 401–406, 2001.
- Charu C Aggarwal, Yan Li, Jianyong Wang, and Jing Wang. Frequent pattern mining with uncertain data. In *Proceedings of the 15th ACM SIGKDD international conference on Knowledge discovery and data mining*, pages 29–38, 2009.
- Barry Becker and Ronny Kohavi. Adult. UCI Machine Learning Repository, 1996. DOI: <https://doi.org/10.24432/C5XW20>.

- Jaewoo Lee and Christopher W Clifton. Top-k frequent itemsets via differentially private fp-trees. In *Proceedings of the 20th ACM SIGKDD international conference on Knowledge discovery and data mining*, pages 931–940, 2014.
- Ricardo Silva Carvalho, Ke Wang, Lovedeep Gondara, and Chunyan Miao. Differentially private top-k selection via stability on unknown domain. In *Conference on Uncertainty in Artificial Intelligence*, pages 1109–1118. PMLR, 2020.
- Tom Fawcett. An introduction to roc analysis. *Pattern recognition letters*, 27(8):861–874, 2006.
- Aaron Roth and Tim Roughgarden. Interactive privacy via the median mechanism. In *Proceedings of the forty-second ACM symposium on Theory of computing*, pages 765–774, 2010.
- Haim Kaplan, Yishay Mansour, and Uri Stemmer. The sparse vector technique, revisited. In *Conference on Learning Theory*, pages 2747–2776. PMLR, 2021.
- Rui Chen, Qian Xiao, Yu Zhang, and Jianliang Xu. Differentially private high-dimensional data publication via sampling-based inference. In *Proceedings of the 21th ACM SIGKDD international conference on knowledge discovery and data mining*, pages 129–138, 2015.
- Ben Stoddard, Yan Chen, and Ashwin Machanavajjhala. Differentially private algorithms for empirical machine learning. *arXiv preprint arXiv:1411.5428*, 2014.
- Reza Shokri and Vitaly Shmatikov. Privacy-preserving deep learning. In *Proceedings of the 22nd ACM SIGSAC conference on computer and communications security*, pages 1310–1321, 2015.
- Mark Bun, Thomas Steinke, and Jonathan Ullman. Make up your mind: The price of online queries in differential privacy. In *Proceedings of the twenty-eighth annual ACM-SIAM symposium on discrete algorithms*, pages 1306–1325. SIAM, 2017.
- Huanyu Zhang, Ilya Mironov, and Meisam Hejzania. Wide network learning with differential privacy. *arXiv preprint arXiv:2103.01294*, 2021.
- Haim Kaplan, Yishay Mansour, Shay Moran, Kobbi Nissim, and Uri Stemmer. On differentially private online predictions. *arXiv preprint arXiv:2302.14099*, 2023.
- Zeyu Ding, Yuxin Wang, Yingtai Xiao, Guanhong Wang, Danfeng Zhang, and Daniel Kifer. Free gap estimates from the exponential mechanism, sparse vector, noisy max and related algorithms. *The VLDB Journal*, 32(1):23–48, 2023.
- David Durfee and Ryan M Rogers. Practical differentially private top-k selection with pay-what-you-get composition. *Advances in Neural Information Processing Systems*, 32, 2019.
- Michael Shekelyan and Grigorios Loukides. Differentially private top-k selection via canonical lipschitz mechanism. *arXiv preprint arXiv:2201.13376*, 2022.
- Gang Qiao, Weijie Su, and Li Zhang. Oneshot differentially private top-k selection. In *International Conference on Machine Learning*, pages 8672–8681. PMLR, 2021.
- Larry Wasserman and Shuheng Zhou. A statistical framework for differential privacy. *Journal of the American Statistical Association*, 105(489):375–389, 2010.
- Zeyu Ding, Daniel Kifer, Thomas Steinke, Yuxin Wang, Yingtai Xiao, Danfeng Zhang, et al. The permute-and-flip mechanism is identical to report-noisy-max with exponential noise. *arXiv preprint arXiv:2105.07260*, 2021.
- Ryan McKenna and Daniel R Sheldon. Permute-and-flip: A new mechanism for differentially private selection. *Advances in Neural Information Processing Systems*, 33:193–203, 2020.
- Craig Cahillane. Sum of exponential and laplace distributions, 2024. URL https://ccahilla.github.io/sum_exponential_and_laplace_distributions.pdf.